Frontiers in Earth Science

TYPE Original Research
PUBLISHED 14 March 2023
DOI 10.3389/feart.2023.1117911

OPEN ACCESS

EDITED BY
Lucja A. Fostowicz-Frelik,
Polish Academy of Sciences, Poland

REVIEWED BY
Grégoire Métais,
Centre National de la Recherche Scientifique (CNRS), France
Takehisa Tsubamoto,
Ehime University, Japan

*CORRESPONDENCE
Bin Bai,
baibin@ivpp.ac.cn

SPECIALTY SECTION
This article was submitted to Paleontology, a section of the journal Frontiers in Earth Science

RECEIVED 07 December 2022
ACCEPTED 27 February 2023
PUBLISHED 14 March 2023

CITATION
Bai B, Wang Y-Q, Theodor JM and Meng J (2023), Small artiodactyls with tapir-like teeth from the middle Eocene of the Erlian Basin, Inner Mongolia, China. *Front. Earth Sci.* 11:1117911.
doi: 10.3389/feart.2023.1117911

Small artiodactyls with tapir-like teeth from the middle Eocene of the Erlian Basin, Inner Mongolia, China

Bin Bai[1]*, Yuan-Qing Wang[1,2], Jessica M. Theodor[3] and Jin Meng[1,4,5]

[1]Key Laboratory of Vertebrate Evolution and Human Origins of Chinese Academy of Sciences, Institute of Vertebrate Paleontology and Paleoanthropology, Chinese Academy of Sciences, Beijing, China, [2]College of Earth and Planetary Sciences, University of Chinese Academy of Sciences, Beijing, China, [3]Department of Biological Sciences, University of Calgary, Calgary, AB, Canada, [4]Division of Paleontology, American Museum of Natural History, New York, NY, United States, [5]Earth and Environmental Sciences, Graduate Center, City University of New York, New York, NY, United States

Artiodactyls diversified during the Eocene and Oligocene in North America and Europe after their first Holarctic appearance at the beginning of the Eocene. However, the relationships among early artiodactyls, European endemic forms, and later derived suiforms, tylopods, and ruminants remain unclear. Early artiodactyls are relatively rare in Asia compared to those known from North America and Europe; thus, investigation of Eocene artiodactyls from Asia is important to resolve these issues. Here we report two new genera and three new species of small early artiodactyls from middle Eocene deposits of the Erlian Basin, Inner Mongolia, China. The new materials represent a morphologically gradational series from Asian Land Mammal Ages Irdinmanhan to Sharamurunian, characterized by a trend towards bilophodonty in the lower molars. Morphologic and phylogenetic analyses suggest that these new taxa have a close relationship with the enigmatic European *Tapirulus*, which currently consists of five species that range from the middle Eocene to the early Oligocene. The close relationship between the Erlian specimens and *Tapirulus* suggests possible faunal exchanges between Europe and Asia during the middle Eocene, a view that has been supported by other mammalian groups across the two continents. The evolution of bilophodonty in Tapirulidae and Raoellidae is probably attributable to convergence.

KEYWORDS

Erlian Basin, Eocene Artiodactyla, Tapirulidae, Homacodontidae, Tethys Sea

1 Introduction

The first appearance of Artiodactyla, Perissodactyla, and Primates in the fossil record marks the Paleocene-Eocene transition when modern mammal orders appeared as archaic groups declined. Asian Paleogene artiodactyls are relatively rare compared to North American and European faunas, and Asian artiodactyls are mostly reported from the Southeast Asia and Indo-Pakistani subcontinent (Theodor et al., 2007). The late middle Eocene Pondaung fauna of Myanmar and the Late Eocene Krabi fauna of Thailand preserve a relatively diverse artiodactyl assemblage, including dichobunids (Métais et al., 2007; Ducrocq et al., 2022), diacodexeids (Ducrocq et al., 2016), anthracotheres (Ducrocq et al., 2001),

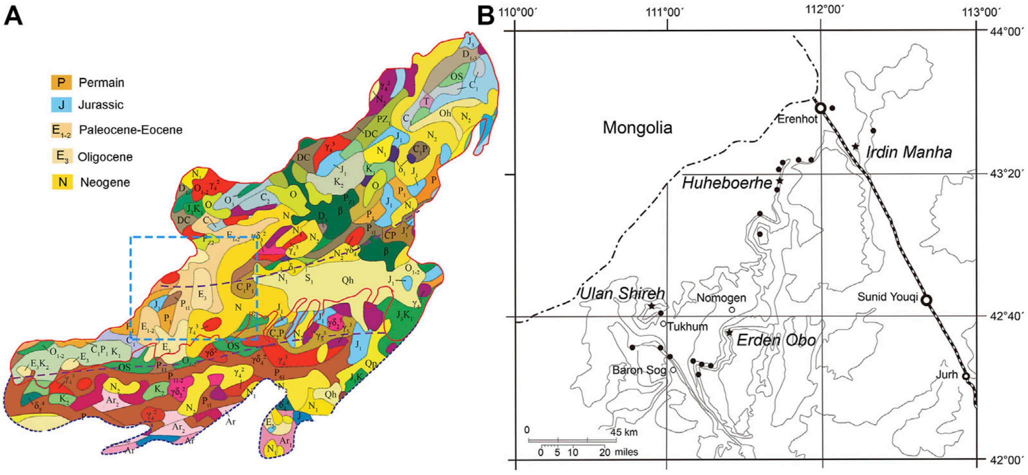

FIGURE 1
Geological map and fossil localities of the Erlian Basin. **(A)** geological map of the Erlian Basin (modified from Zhang et al., 2019, Fig. 3, with permission from S. Fu); **(B)** Paleogene fossil localities in the Erlian Basin with solid stars indicating the localities where new artiodactyl fossils were unearthed (modified from Bai et al., 2018, Fig. 1).

ruminants (Métais et al., 2000; Métais et al., 2001; Métais, 2006; Ducrocq et al., 2020), and some indeterminate groups (Tsubamoto et al., 2013). Early and middle Eocene artiodactyls from Indo-Pakistan include diacodexeids, dichobunids, and endemic raoellids (Theodor et al., 2007; Thewissen et al., 2020). A few diacodexeids, dichobunids, helohyids, and controversial raoellids are known from the middle Eocene of Andarak 2, Kyrgyzstan (Averianov, 1996), Chakpaktas Svita of Kazakhstan (Gabunia, 1971; Gabunia, 1973), and Khaichin-Ula II of Mongolia (Vislobokova, 2004a; Vislobokova, 2004b; Vislobokova, 2004008; Orliac and Ducrocq, 2012). The Eocene mammal faunas from China are dominated by diverse perissodactyls (Bai et al., 2020), however, artiodactyls from the middle Eocene Shanghuang fissure-fillings of Jiangsu Province are more diverse and abundant than in contemporary Chinese faunas. *Elaschitotherium*, the homacodontid *Limeryx*, diacodexeids such as *Jiangsudon*, and indeterminate suoids have been reported from Shanghuang fissures (Métais et al., 2004; Métais et al., 2005; Métais et al., 2008; Orliac and Ducrocq, 2012).

The Erlian Basin is located in the south of the Mongolia Plateau and at the junction between the North China Block and the Siberian Plate (Zhang et al., 2019; Fu et al., 2021). The continental Mesozoic and Cenozoic sediments are widely distributed in the Erlian Basin, including the nearly continuous Paleogene deposits bearing abundant mammalian fossils (Figure 1), which form the basis of the Eocene Asian Land Mammal Ages (Wang et al., 2012; Wang et al., 2019). Artiodactyl fossils have been reported from the Erlian Basin since the Central Asiatic Expedition (CAE) by the American Museum of Natural History in the 1920s, including *Gobiohyus*, *Erlianhyus*, and an achaenodont from the Irdin Manha Formation (Matthew and Granger, 1925a; Coombs and Coombs, 1977; Li and Li, 2021), *Archaeomeryx* from the Shara Murun Formation (Matthew and Granger, 1925b; Vislobokova, 2002), *Entelodon* from the Houldjin and upper Naogangdai formations (Matthew and Granger, 1923; Jiang, 1983; Lucas and Emry, 1996; Wang et al., 2009), and *Brachyhyops* from the "Ulan Gochu Formation" at Twin Oboes (Wang and Qiu, 2002). We report new artiodactyl material with lophodont-like teeth from the middle Eocene of the Erlian Basin, Inner Mongolia, the first small, basal artiodactyls from the Erlian Basin since the CAE expedition. This material shows striking similarities with the enigmatic European *Tapirulus*, supporting faunal exchange between Europe and Asia during the early middle Eocene. In addition, we discuss the unusual evolution of bilophodonty in artiodactyls.

2 Materials and methods

Several isolated teeth, fragmentary low jaws, and a calcaneus were recovered from the Irdin Manhan Formation at Irdin Manha and Huhoboerhe, a right lower jaw with p4–m3 from the upper part of the "Basal White" at Erden Obo (Urtyn Obo), and a left lower jaw with m2–3 from the base of the Shara Murun Formation at Ula Usu (Figure 1). A left lower jaw with m1 talonid, m2–3, and a left astragalus are probably from the Ulan Shireh Formation at North Mesa, but their specific horizon and locality remain uncertain.

Phylogenetic analyses were conducted using the parsimony Traditional Search method in TNT 1.5 (Goloboff et al., 2008; Goloboff and Catalano, 2016). The data matrix used in the analyses, modified from the data of Métais et al. (2004), contained a total of 31 taxa and 34 dental characters. All characters were equally weighted, and four characters (3, 7, 8, 13) were ordered. The heuristic search algorithm was used with 1,000 replications of random stepwise addition and tree-bisection-reconnection (TBR) branch swapping. Then the Traditional Search was again conducted on trees from RAM because some replications overflowed. Branches were collapsed when their minimum length was equal to zero.

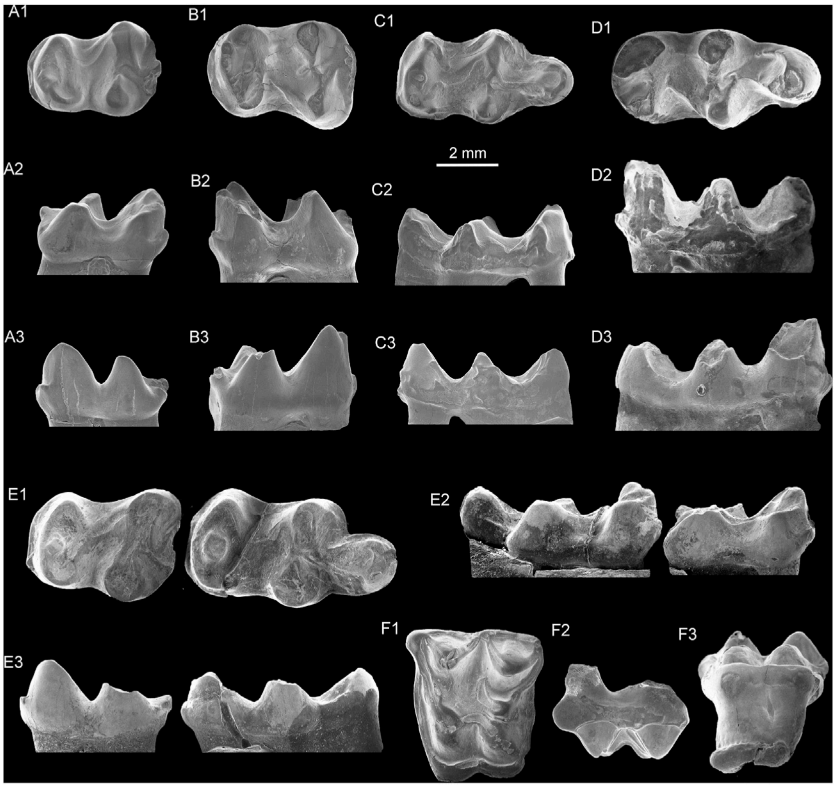

FIGURE 2
Lower molars of *Obotherium parvum* gen. et sp. nov. **(A–E)** and the upper molar of ? *Obotherium parvum* **(F)**. **(A)** right m1/2 (holotype, IVPP V 31726); **(B)** left m1/2 (V 31727.1); **(C)** right m3 (V 31727.2); **(D)** left m3 (V 31728.1); **(E)** right m2–3 (V 31729); **(F)** left M1/2 (IVPP V 31730): **(A1–F1)**, occlusal view; **(A2–F2)**, buccal view; **(A3–F3)**, lingual view.

3 Systematic paleontology

Order ARTIODACTYLA Owen, 1848
Family TAPIRULIDAE Cope, 1879
Type genus—*Tapirulus* Gervais, 1850
Included genera—type genus, *Obotherium* gen. nov., and *Tapiruloides* gen. nov.

Diagnosis—Small artiodactyls with a flat, narrow, elongated skull with reduced mastoid and relatively longer preorbital portion, without preorbital fossa; relatively wide but short brain; neopallium only slightly differentiated; dentition bilophodont in derived forms; lower molars with a transversely extended posthypocristid, a more or less complete hypolophid, an elongated, well-developed hypoconulid on m1–2, and m3 hypoconulid enlarged into a third lobe; premolars, canine, and incisors in continuous series without diastema (modified from Sudre, 1978; Erfurt and Métais, 2007).

Age and distribution—Middle Eocene to early Oligocene of Europe and Middle Eocene of Asia.

Obotherium gen. nov.
Type species—*Obotherium parvum* sp. nov.
Etymology—Obo, a pile of rocks with wood often found on the top of mesas for Heaven-worship ceremonies; Latin, *-therium*, beast.
Included species—Type and *Obotherium tongi* sp. nov.
Diagnosis—Lower molars with anteroposteriorly compressed trigonid, talonid wider than trigonid, entoconid slightly more anteriorly placed to hypoconid, and cristid obliqua extended to the point buccal to the midpoint of the protocristid; p3 trenchant, p4 with well-developed metaconid and distinct paraconid.
Differential diagnosis—Differs from *Tapirulus* by an entoconid more anteriorly placed to the hypoconid on the lower molars, and premolars less elongated. Differs from *Tapiruloides* by an anteriorly slanted trigonid, a less complete hypolophid, a distinct cristid obliqua on the lower molars, and a less sharp hypoconulid on m3.
Age and distribution—Middle Eocene of Asia.

Obotherium parvum sp. nov.
(Figures 2A–E; Table 1)
Holotype—IVPP V 31726, a right m1/2 (Figure 2A).
Etymology—Latin, *parvus*, little; in allusion to its small size.
Type locality and horizon—Irdin Manha Formation, Irdin Manha, Erlian Basin (field no. 11107). Irdinmanhan ALMA.
Paratype—IVPP V 31727.1–.2 (Figures 2B, C), a left m1/2 and a right m3 (field no. 11377); IVPP V 31728.1 (Figure 2D), a fragmentary lower jaw with a left m3 (field no. 11155). All from Irdin Manha Formation at Irdin Manha.

TABLE 1 Measurements of the lower molars of *Obotherium* and *Tapiruloides* (in mm) (*: approximate value).

		m1/2 L	m1/2 AW	m1/2 PW	m3 L	m3 AW	m3 PW
Obotherium parvum	V 31726 (holotype)	4.30	2.52	3.10			
	V 31727.1–.2	4.50	3.12	3.55	5.65	2.80	3.00
	V 31728.1				6.21	2.95	3.10
	V 31729	4.80	3.11	3.68	6.90	3.50	3.60
Obotherium aff. *O. tongi*	V 31732.1	4.82	3.15	3.50	5.91	3.10	3.30
	V 31733				5.80	2.95	3.10
	V 31734				5.90	2.98	3.12
Obotherium sp. 1	V 31735	4.30	2.50	2.89			
Obotherium sp. 2	V 31736	4.60	2.61	3.00			
Tapiruloides usuensis	V 31737 (holotype)	5.60	3.30*	3.81	6.52	3.22	3.21

Referred specimen—IVPP V 31729 (Figure 2E), a right lower jaw with m2–3, Irdin Manha Formation at Huheboerhe (field no. HIL082–1).

Differential diagnosis—Differs from *Obotherium tongi* by a less anteroposteriorly compressed trigonid with a reduced paraconid, a less complete hypolophid composed of postentocristid and posthypocristid, a bifurcated posthypocristid with one branch descending to hypoconulid on m1-2, a less posteriorly extended hypoconulid on m1-2, and a prehypoconulid cristid of m3 joining the posthypocristid.

3.1 Description

Four fragmentary lower jaws, each bearing a single molar, and a right lower jaw with m2–3 are referred to *Obotherium parvum*. The hypoconulid on IVPP V 31726, the protoconid and entoconid on V 31727.1, and nearly all tips of the cuspids show partial breakage, except the hypoconid on V 31728.1.

The trigonid of m1/2 is anteroposteriorly compressed with the metaconid lingual to the protoconid. The protoconid and hypoconid are lower than the metaconid and entoconid, respectively. The protocristid is more heavily worn on the posterior wall than the paracristid on the holotype. The paracristid is slightly notched with an indistinct paraconid on the holotype or a small one anterobuccally placed to the protoconid on the paratype. The talonid is considerably wider, longer, and slightly lower than the trigonid. The hypoconid is more buccally placed than the protoconid, extending a cristid obliqua anterolingually to the base and slightly buccal to the midpoint of the protocristid. The entoconid is slightly more anteriorly placed than the hypoconid. The hypolophid of the preultimate molar is somewhat interrupted at the conjunction of posthypocristid and postentocristid, and the postentocristid is transversely extended. The posthypocristid is nearly transversely extended and diverges into two ridges near its lingual extremity: one descends posteriorly to the hypoconulid, and another short one is anterolingually extended, joining the postentocristid. Although the hypoconulid is partially broken on both V 31726 and V 31727.1, it is a low cuspid rising from a distinct postcingulid, slightly lingually placed to the median of the posterior border, and does not expand posteriorly. The precingulid is relatively weaker than the postcingulid, while the buccal and lingual cingulids are absent.

The m3 is similar to m1/2 in morphology but differs from the latter in having a talonid slightly wider than the trigonid, an entoconid nearly lingually placed to the hypoconid, and the hypoconulid enlarged into a third lobe. The transverse posthypocristid slightly posteriorly descends to the median between the hypoconid and entoconid, where it joins the distinct prehypoconulid cristid. The hypoconulid lobe is relatively long and high. A ridge along the lingual border of the hypoconulid lobe is distinct on V 31728.1, weak on V 31727.2, and nearly absent on V 31729. The buccal cingulid at the base of the hypoconulid lobe is weak or absent. A weak precingulid is present as in m1/2.

3.2 Comparisons

With Homacodontidae—Among early artiodactyls, *Obotherium* is more similar to the mainly Homacodontidae and Dichobunidae; however, both are considered to be paraphyletic. The early Eocene *Hexacodus* from the North American Wasatchian was initially only known from two lower jaws representing two species, *H. pelodes* and *H. uintensis* (Gazin, 1952). Gazin (1962) assigned several upper cheek teeth and a lower jaw to *Hexacodus* cf. *H. pelodes*. The genus *Hexacodus* is probably paraphyletic (Gazin, 1962; Stucky, 1998). *Obotherium parvum* is similar to *Hexacodus pelodes* in having: 1) an anteroposteriorly compressed trigonid on the lower molars with the paraconid closely appressed to the metaconid; 2) the metaconid lingual to the protoconid; 3) the talonid wider than the trigonid on m1-2; and 4) the posthypocristid transversely extended with its lingual end sending a weak spur posteriorly to the hypoconulid. The lower molars of *Hexacodus pelodes* differ from those of *Obotherium parvum* in having the cristid obliqua more lingually extended to the midpoint of the protocristid, the isolated entoconid lingual to the hypoconid without the postentocristid (m2 likely with a short postentocristid on USNM 19215), hypoconulid more lingually placed, distinct buccal cingulids, and m3 hypoconulid much smaller.

The early-middle Eocene homacodontids from the North American Bridgerian are represented by small *Microsus* and relatively larger *Homacodon* (Stucky, 1998), similar to *Obotherium parvum* in having above characters 1–3. *Microsus* resembles *Obotherium parvum* in having a transversely extended posthypocristid on the lower molars and the postentocristid of m2 joining posthypocristid (Sinclair, 1914, fig. 22–23). *Microsus* sp. (USNM 364914 and other USNM specimens) has a hypolophid that connects hypoconid and entoconid, and a strongly developed prehypoconulid cristid intersecting the posthypocristid at a 90° angle (Stucky, 1998); the relatively complete hypolophid in *Microsus* sp. is similar to *Obotherium parvum*. The lower molars of *Homacodon* have bunodont lingual cuspids and buno-selenodont buccal cuspids with posthypocristid posterolingually directed to the hypoconulid (Sinclair, 1914), unlike the transversely extended posthypocristid in *Obotherium*, *Hexacodus*, and *Microsus*. However, the hypoconulid of m1-2 in *Homacodon* is nearly medially placed on the postcingulid as in *Obotherium parvum*.

The North American Uintan homacodontids, including *Bunomeryx*, *Hylomeryx*, *Pentacemylus*, *Mytonomeryx*, and *Mesomeryx*, are separated from other homacodontids as a family Bunomerycidae by Gentry and Hooker (1988). The relationship between Uintan homacodontids and later artiodactyls is controversial in that some genera are probably closely related to Tylopoda, while others are close to Ruminantia (Stucky, 1998; Norris, 1999). The lower molars of Uintan homacodontids differ from *Obotherium parvum* in their preselenodont condition: paracristid deeply but narrowly notched (Gentry and Hooker, 1988), cristid obliqua more lingually extended, and hypoconid selenodont with posthypocristid usually posterolingually extended to the lingually placed hypoconulid (Gazin, 1955). *Mesomeryx* is as small as *Microsus cuspidatus* and is known from the upper teeth (Peterson, 1919; Gazin, 1955). The lower molars of *Bunomeryx* differ from those of other Uintan homacodontids in that the posthypocristid is more transversely extended and descends posteriorly at an angle to behind the entoconid (Stucky, 1998), and a weak cristid present on the buccal surface of the entoconid on m1-2 as in *Obotherium parvum*. However, the hypoconulid of m1-2 in *Obotherium parvum* is more medially placed. *Hylomeryx* comprises two species *H. annectens* and *H. quadricuspis* (Peterson, 1919; Gazin, 1955). The lower cheek teeth of *H. quadricuspis* (CM 2346) are heavily worn and crescentic, but the conditions in *H. annectens* are confusing. The holotype of *H. annectens* (CM 2335) has a transversely extended hypolophid more distinct than a weak posthypocristid on m1-2 (Peterson, 1919, Pl. 36, Fig. 6), whereas the paratype of *H. annectens* (CM 2944) has a distinct crescentic hypoconid with the distinct posthypocristid posterolingually extended on m1-3 (Peterson, 1919, Fig. 10). In general, *Obotherium parvum* is similar to Uintan homacondontids in having a small size, enlarged hypoconulid lobe on m3, and crescentic hypoconid on the lower molars. However, *Obotherium parvum* shows some more basal characters on the lower molars: a complete or shallowly notched paracristid, a more distinct paraconid, and the talonid considerably wider than the trigonid.

Limeryx and *Asiohomacodon* from Asia were provisionally assigned to Homacodontidae or Homacodontinae (Tsubamoto et al., 2003; Métais et al., 2005; Theodor et al., 2007), and they show bunoselenodont or fully selenodont teeth which differ from *Obotherium parvum*.

With Dichobunidae—Dichobunidae is composed of four subfamilies: Dichobuninae, Eurodexeinae, Lantianiinae, and Hyperdichobuninae (Theodor et al., 2007). Dichobuninae is restricted to Europe from the early Eocene to the late Oligocene, and is generally more bunodont than *Obotherium parvum* (Theodor et al., 2007). Oligocene dichobunines *Synaphodus* and *Metriotherium* with selenodont dentition are considerably larger than *Obotherium parvum*, although a lophid-like cristid joins the hypoconid and entoconid on the lower molars in *Metriotherium* (Lavocat, 1951; Theodor et al., 2007). The lower molars of Eocene dichobunines differ from those of *Obotherium parvum* by larger size, more bunodont teeth, and smaller and shorter hypoconulid on m3. *Messelobunodon* is further distinguished by an isolated paraconid on the lower molars, and *Neufferia* is characterized by the hypoconid and entoconid divided by a deep valley without hypoconulid (Franzen, 1981; Franzen, 1994; Theodor et al., 2007). *Dichobune* is comprised of five species ranging from the middle Eocene to the early Oligocene (Theodor et al., 2007). *Dichobune* differs from *Obotherium parvum* by the rounded, more or less isolated metaconid and entoconid, crescentic protoconid and hypoconid, a weak ridge between the hypoconid and the entoconid (in *Dichobune jehenni* and *D. leporinum*), and the hypoconulid distinct or absent (in *D. leporinum*) (Stehlin, 1906; Sudre, 1978; Brunet and Sudre, 1980; Hooker and Weidmann, 2000).

Eurodexeinae comprises four genera (*Eygalayodon*, *Lutzia*, *Eurodexis*, and *Parahexacodus*) and ranges from the late early Eocene to early middle Eocene (MP10 to MP13 or 14) in Europe (Erfurt and Sudre, 1996; Theodor et al., 2007). This group is similar to North American basal homacodontids and *O. parvum* in having a small size, anteroposteriorly compressed trigonid with reduced paraconid on the lower molars, and the posthypocristid transversely extended joining the postentocristid if present (Sudre and Erfurt, 1996). However, these are probably a result of similar ecological adaptation, and eurodexeines are rooted in the European stock of *Diacodexis* (Sudre and Erfurt, 1996; Theodor et al., 2007). Lower molars of Eurodexeinae differ from those of *Obotherium parvum* in having trigonid much higher than the talonid, talonid lingually enclosed by the preentocristid (in *Eurodexis*, *Parahexacodus*, and *Eygalayodon*), entoconid lingual or posterior to the hypoconid, posthypocristid not bifurcated, and m3 hypoconulid relatively small but stout (Sudre and Erfurt, 1996; Theodor et al., 2007).

The middle-late Eocene Hyperdichobuninae is comprised of *Hyperdichobune* and *Mouillacitherium*, and represents a poorly known miniature, primitive group (Gentry and Hooker, 1988; Hooker and Weidmann, 2000; Theodor et al., 2007). *Hyperdichobune* comprises five species known from MP13 to MP 19 (Theodor et al., 2007), and four species of the genus were initially assigned to *Dichobune* (Stehlin, 1906; 1910). The lower molars of *Hyperdichobune* show some similarities with those of *Obotherium parvum* in having a talonid wider than trigonid (in *H. langi*), entoconid slightly more anteriorly placed to the hypoconid (in *H. langi* and *H. nobilis*), a connection between the hypoconid and entoconid on m2 (in *H. nobilis*), and enlarged hypoconulid lobe on m3 (Stehlin, 1906; 1910; Sudre, 1972). The lower molars of *Hyperdichobune* mainly differ from those of *Obotherium parvum* in having an isolated, rounded entoconid, relatively weak crescentic hypoconid with posthypocristid directly joining the hypoconulid (Stehlin, 1906; 1910; Sudre, 1972). *Mouillacitherium* comprises three species that form a lineage from *M. cartieri via M. schlosseri* to *M. elegans*, and ranges from MP14 to MP18 (Sudre, 1978; Theodor et al., 2007). The lower molars of *Mouillacitherium* mainly differ from those of *Obotherium parvum* in having acute metaconid and entoconid, crescentic protoconid and hypoconid, and distinct preentocristid and postmetacristid, although there is a tendency to form a connection between the hypoconid and entoconid in *Mouillacitherium* (Stehlin, 1906; Stehlin, 1910; Sudre, 1978).

Lantianiinae is restricted to the middle Eocene of Asia, comprising *Lantianius, Eolantianius*, and *Elaschitotherium* (Métais et al., 2004; Theodor et al., 2007). *Elaschitotherium* is known from the middle Eocene Shanghuang fissure-filling of Jiangsu, China (Métais et al., 2004; Métais et al., 2008). The lower molars of *Elaschitotherium* are similar to those of *Obotherium parvum* in having an anteroposteriorly compressed trigonid on m2-3, the talonid wider than the trigonid, the entoconid slightly anterior to the hypoconid, a transversely extended posthypocristid, and a cristid obliqua more buccally extended. The lower molars of *Elaschitotherium* differ from those of *Obotherium parvum* in having a conical, isolated entoconid, a slightly transversely compressed metaconid, an incipient preentocristid (in *E. crepaturus*), more lingually placed hypoconulid on m1-2, and a relatively smaller m3 hypoconulid. The m1 of *Elaschitotherium qii* (IVPP V 12759.47) varies in possessing a complete hypolophid as in *Obotherium parvum* (Métais et al., 2004, Fig. 2G), but the former has a deeply notched hypolophid to which the prehypoconulid cristid is directly oriented.

Eolantianius russelli known from the middle Eocene Andarak 2, Kyrgyzstan is represented by DP4 and upper molars (Averianov, 1996; Averianov and Godinot, 2005), showing a striking resemblance to *Elaschitotherium qii* (Métais et al., 2004). An isolated m2 and m3, tentatively assigned to ? *Eolantianius russelli* by Averianov (1996), are very similar to those of *Obotherium parvum* in a smaller size, a reduced paraconid, a talonid wider than the trigonid, a more buccally directed cristid obliqua, entoconid anterior to hypoconid, nearly complete hypolophid, transversely extended posthypocristid, a large, medially placed hypoconulid joining the posthypocristid by a cristid, and an enlarged hypoconulid lobe on m3. However, m2-3 of ?*Eolantianius russelli* differs from *Obotherium parvum* by a less compressed trigonid. Absent the upper molar of ? *Obotherium parvum* described below, we might have assigned the lower dentition from the Erlian Basin to ? *Eolantianius;* however, it is uncertain whether m2-3 of ? *Eolantianius russelli* was unearthed from the same horizon as the upper molars from Andarak II (Russell and Zhai, 1987). It seems likely that the lower molars assigned to ? *Eolantianius russelli* represent a different taxon from the uppers of *Eolantianius russelli*, and should be transferred to *Obotherium*.

With *Tapirulus*—*Tapirulus* is a European artiodactyl known from the middle Eocene to the early Oligocene (Erfurt and Métais, 2007), *Tapirulus* currently consists of five species that succeed each other in a chronocline and is characterized by its bilophodont tooth pattern (Stehlin, 1910; Sudre, 1978; Hooker and Weidmann, 2000; Erfurt and Métais, 2007). Its phylogenetic position is controversial, and the genus has been included in Dacrytheriinae (or Dacrytheriidae) (Viret, 1961; Sudre, 1978; McKenna and Bell, 1997), a tylopod *incertae sedis* (Hooker and Weidmann, 2000), or Choeropotamidae (Hooker and Thomas, 2001; Erfurt and Métais, 2007). *Tapirulus majori* (MP13) and *T. depereti* (MP 14) are fragmentary, but the lower molars are strikingly similar to *Obotherium parvum,* having an anteroposteriorly compressed trigonid with a reduced paraconid, an incomplete transverse ridge between the hypoconid and entoconid, a posthypocristid descending a cristid to a relatively distinct hypoconulid, and the talonid slightly wider than the trigonid (Stehlin, 1910). However, the hypoconulid is more posteriorly extended in *Tapirulus majori*, *T. depereti* than in *Obotherium parvum*, and the former two species have the entoconid nearly lingual to the hypoconid (Stehlin, 1910, Pl. 19, fig. 24, 30). These two characters are consistent with later species of *Obotherium* described below. The lower molars of *Tapirulus schlosseria* from MP 16 have a second ridge rising from the hypoconulid to the hypolophid (Stehlin, 1910, p. 1075), somewhat reminiscent of those of *Obotherium parvum*. Late middle Eocene–early Oligocene *Tapirulus perrierensis* and *T. hyracinus* are characterized by more bilophodont teeth (Stehlin, 1910; Sudre, 1978), nearly identical to the new material of a left lower jaw with m2-3 (IVPP V 31737) from Ula Usu described below.

Obotherium parvum is more similar to *Tapirulus majori* and *T. depereti* than to any other early artiodactyls, suggesting a close relationship. Both *Obotherium* and *Tapirulus* likely descended from early North American homacodontids. The new species is assigned to a new genus *Obotherium* rather than to *Tapirulus*, because the differences between the new species and the type species of *Tapirulus* (T. *hyracinus*) warrant generic distinction; it is possible that *Tapirulus majori* and *T. depereti* differ from other species of *Tapirulus* at the generic level (Stehlin, 1910) and are more reasonably included in *Obotherium*.

? *Obotherium parvum*

Material—IVPP V 31730, a left M1 (Figure 2F).

Locality and horizon—Irdin Manha Formation, Irdin Manha escarpment (field no. 13054), Erlian Basin.

3.3 Description

The M1 is quadrate in outline and brachydont (Length: 4.40 mm; Anterior Width: 4.90 mm; Posterior Width: 4.65 mm). The ectoloph is W-shaped with a buccally flexed centrocrista. The preparacrista extends from the paracone to the posterobuccal side of the parastyle. The parastyle is distinct and anteriorly projected, while the mesostyle is weak and represented by a bulge from the cingulum. The metastyle is absent. The metacone is slightly larger and more lingually appressed than the paracone. The buccal surfaces of the paracone and metacone are nearly flat, and a faint rib is present on the metacone. The protocone is at the level of the paracone without a postprotocrista. The paraconule is small, indistinct, and closer to the protocone than to paracone. The protoloph, composed of preprotocrista and preparaconule crista, is complete and joins the

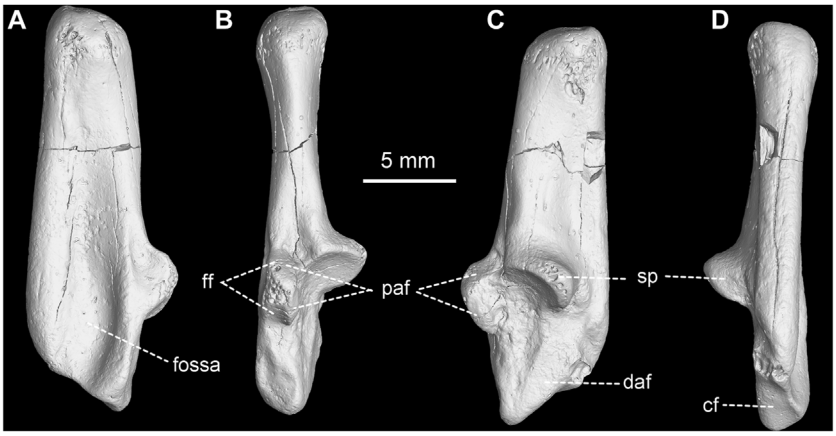

FIGURE 3
Right calcaneus of Tapirulidae gen. et sp. indet. (IVPP V 31728.2). **(A)** lateral view; **(B)** anterior view; **(C)** medial view; **(D)** posterior view. Abbreviation: *cf*, cuboid facet; *daf*, distal astragalar facet; *ff*, fibular facet; *paf*, proximal astragalar facet; *sp*, sustentacular process.

parastyle. The hypocone is large and conical, slightly more lingually placed than the protocone, and more anteriorly situated than the metacone. A well-developed prehypocrista extends anterobuccally from the hypocone to the middle valley, then curves towards the protocone for a short distance before joining the apex of the protocone, enclosing the lingual opening of the middle valley. The metaconule is crescentic and separated from the hypocone by a narrow groove. The premetaconule crista extends from the metaconule to the anterolingual base of the metacone; the postmetaconule crista is longer and joins the postmetacrista at the base. The cingula are complete and continuous around the anterior, lingual, and posterior bases of the crown with the lingual one relatively stronger. Worn facets are present along the postcingulum, the buccal half of the precingulum, and the middle of the lingual cingulum. The buccal cingulum is complete and weak.

3.4 Comparisons

The morphology of this isolated upper molar shows some similarities with Uintan homacodontids, including a quadrate outline of the crown, selenodont, a W-shaped ectoloph, a well-developed hypocone on M1 and/or M2 (except *Mesomeryx* and *Pentacemylus*), and a selenodont metaconule (Gazin, 1955). The reduced paraconule and weak mesostyle in IVPP V 31730 are more similar to *Hylomeryx* than to other Uintan homacodontids, but *Hylomeryx* has a more bunodont paracone and metacone on the upper molars (Peterson, 1919; Gazin, 1955). The upper molars of Wasatchian and Bridgerian *Hexacodus* cf. *H. pelodes*, *Microsus*, and *Homacodon* are distinguished from V 31730 by more bunodont dentition, straight centrocrista, and relatively large paraconule (Gazin, 1955; Gazin, 1962; West, 1984). V 31730 is unique in having a prehypocrista towards the protocone and partially enclosing the talon lingually; similarly, the incipient hypocone rising from the cingulum on M2 of *Hexacodus* cf. *H. pelodes* also extends a slight crest toward the protocone (Gazin, 1962).

The combination of W-shaped ectoloph, well-developed hypocone, a quadrate outline of the crown, and lack of postprotocrista toward the metaconule in V 31730 is distinguishable from Dichobunidae (Erfurt and Métais, 2007; Theodor et al., 2007). *Dichobune*, with quadrate outline and distinct hypocone on the upper molars, also differs from V 31730 in having the protoloph descending towards the anterior cingulum before reaching the anterobuccal corner of the crown (Sudre, 1978). Although the upper molars of Lantianiinae are clearly different from V 31730, *Eolantianius* is more similar to V 31730 in having a subquadrate outline of the crown, distinct parastyle, and a faint paraconule without a postparaconule crista than *Elaschitotherium* (Averianov, 1996; Métais et al., 2004). However, these similarities are more probably attributable to parallel evolution rather than a close phylogenetic relationship, considering the bunodont paracone and metacone and straight ectoloph in *Eolantianius*.

The upper molars of *Tapirulus majori*, *T. depereti*, and *T. schlosseri* from MP13 to MP16 are rare and mostly known from isolated teeth, however, *Tapirulus perrierensis* and *T. hyracinus* from late Eocene to the early Oligocene are known from complete maxilla and skull (Stehlin, 1910; Sudre, 1978; Erfurt and Métais, 2007). *Tapirulus majori* and *T. depereti* resemble V 31730 in having a distinct parastyle, relatively weak paraconule on the upper molars, and crescentic metaconule. *Tapirulus depereti* is similar to V 31730 in having a W-shaped ectoloph on the upper molars, while the centrocrista of the upper molar is nearly straight or slightly buccally flexed in *T. majori* (Stehlin, 1910). *Tapirulus schlosseri*, *T. perrierensis* and *T. hyracinus* possess W-shaped ectoloph on the upper molars, but they are distinguished by the advanced bilophodont dentition with compressed, transversely extended protoloph and metaloph (Stehlin, 1910). The most conspicuous difference between V 31730 and the middle Eocene *Tapirulus* is the lack of hypocone on the known upper molars in *Tapirulus*. However, the upper molars of the middle Eocene *Tapirulus* are fragmentary and only known from M2 or M3, and it is possible that M1 possesses a distinct hypocone as in V 31730 since the hypocone can be very

FIGURE 4
Right lower jaw of *Obotherium tongi* gen. et sp. nov. with p3-m3 and alveoli of canine, p1, and root of p2 (IVPP V 31731). **(A)** occlusal view; **(B)** buccal view; **(C)** lingual view.

variable on different molars. The M1 hypocone is well-developed but absent or highly reduced on M2–3 in *Bunomeryx*, while it is present on M1–2 but absent on M3 in *Homacodon*, *Microsus*, *Hylomeryx*, and *Mytonomeryx* (Gazin, 1955; Theodor et al., 2007).

The specimen V 31730 was also discovered from the Irdin Manha Formation at Irdin Manha as the holotype and paratype of *Obotherium parvum*. They both have a similar evolutionary level with the Uintan homacodontids and strikingly resemble *Tapirulus*, indicating V 31730 probably represents the upper molar of *Obotherium parvum*. However, pending the discovery of more material of the upper cheek teeth of this small artiodactyl, we tentatively assigned the specimen to *Obotherium parvum* with a question mark.

Gen. et sp. indet.

Material—IVPP V 31728.2 (Figure 3), a left calcaneus from the Irdin Manha Formation at Irdin Manha (field no. 11155).

3.5 Description

The calcaneus is discovered from the same pit as V 32728.1, a left lower jaw with m3 of *Obotherium parvum*, so it may belong to *O. parvum* considering their comparable small size. The calcaneus (IVPP V 31728.2) is strongly lateromedially compressed (Figure 3). The lateral surface of the calcaneus has a moderately deep fossa on the distal two-thirds length presumably for the attachment of the calcaneofibular ligaments. The fibular facet on the ectal process is proximodistally convex with the long axis parallel to that of the calcaneus. However, its proximal half is confluent with astragalar facet and seems very narrow. The proximal astragalar facet is composed of two parts: one on the medial side of the distal half of the fibular facet, and the other occupies the proximal surface of the ectal process. A shallow fossa is present proximal to the ectal process. There is a flat, triangular distal astragalar facet on the medial side of the calcaneus. The sustentacular process is weakly medially projected with a rounded, concave facet, which is oriented more distally than anteriorly. The sustentacular facet is continuous with the medial surface of the ectal process. Distally, the cuboid facet is narrow, flat, and distoposteriorly directed.

Calcaneus Measurements (mm): Length=21.80; Proximal width=3.93; Minimum width of shaft=2.47; Width at sustentaculum=5.40; Distal width=2.72; Dorsoplantar depth of tuber=4.93; Depth at ectal process=8.07; Depth at distal end=6.14.

3.6 Comparisons

This calcaneus is compared with *Diacodexis* and *Bunophorus* (Guthrie, 1968; Kumar et al., 2010). This calcaneus differs from

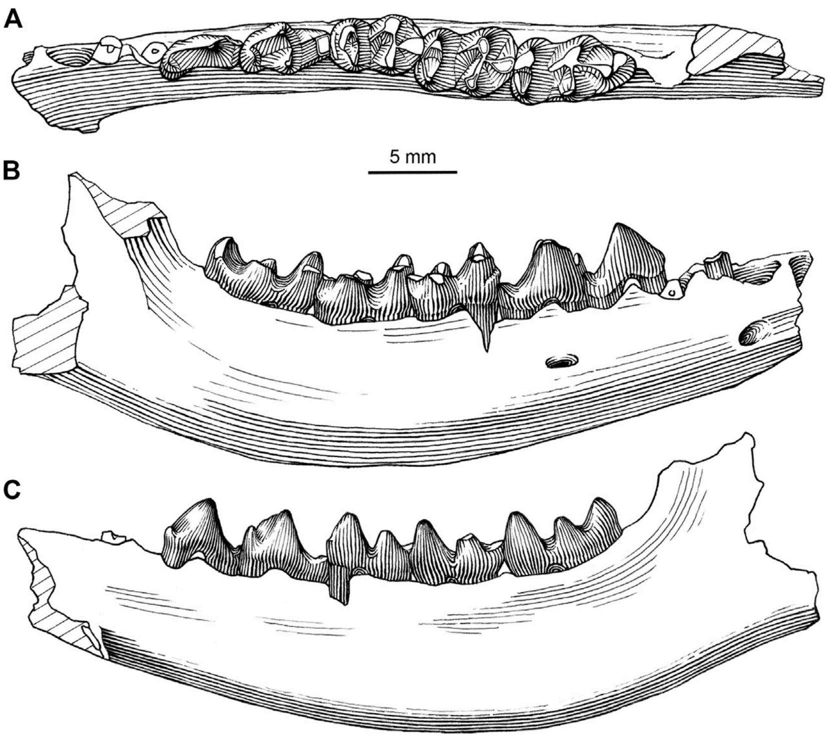

FIGURE 5
Line drawing of the right lower jaw of *Obotherium tongi* gen. et sp. nov. with p3-m3 and alveoli of canine, p1, and root of p2 (IVPP V 31731). **(A)** occlusal view; **(B)** buccal view; **(C)** lingual view.

Diacodexis and *Bunophorus* by a relatively longer calcaneal tuber, a less medially projected sustentaculum, nearly confluent astragalar and fibular facets on the proximal half of the ectal process (Guthrie, 1968; Kumar et al., 2010). The calcaneus of *Diacodexis* has a relatively deeper fossa on the lateral side and a more distinct peroneal process than IVPP V 31728.2 (Kumar et al., 2010).

Obotherium tongi sp. nov.
(Figures 4, 5; Table 2)
Holotype—IVPP V 31731, a nearly complete right lower jaw with p3-m3.
Etymology—Named in honor of Prof. Yong-Sheng Tong for his contribution to the Paleogene mammals from China.
Differential diagnosis—Differs from *Obotherium parvum* by a more anteroposteriorly compressed trigonid without a paraconid, a more complete hypolophid with a long prehypoconulid cristid joining the middle of the hypolophid on m1-2 or directed to the lingual side of the hypoconid on m3, and a more posteriorly extended hypoconulid on m1-2.
Type locality and horizon—the upper part of the “Basal White” layer at Erden Obo (field no. 10227), Erlian Basin. Irdinmanhan ALMA.

3.7 Description

The horizontal mandibular ramus is slender and relatively shallow with a convex ventral border. The depth of the horizontal ramus is nearly consistent and becomes slightly shallower anteriorly. Two mental foramina are preserved: The anterior one is rounded, below p1, while the posterior one is elongated and below p4. The posterior border of the symphysis is at about the level of the anterior border of the p2.

The lower canine and the cheek teeth are closely spaced without diastema. The partial canine alveolus is preserved and nearly vertical, indicating canine is larger than p1. The alveolus of p1 is a relatively large anteroposteriorly elongated oval. The p2 preserves two roots with the posterior one situated anterobuccal rather than anterior to the p3 paraconid. The crown of p3 is laterally compressed and composed of a main, sharp cuspid. Two cristids descend from the main cuspid: a short, slightly convex anterior one descends to a faint paraconid, while a long, slightly concave one terminates in a low, distinct hypoconid. The cingulid is absent on p3.

The trigonid of p4 is wider, longer, and higher than the talonid. The metaconid is as large as the protoconid, lingually and slightly posteriorly situated to the latter. The protocristid, the widest portion of the crown, is moderately notched. The paracristid is distinct, nearly anteriorly extended from the protoconid. The paraconid is prominent and medially placed, separated from the paracristid by a relatively deep notch. The talonid tapers posteriorly and its posterolingual part is broken. The buccally placed hypoconid seems more distinct than that of p3. The feeble cristid obliqua ascends from the hypoconid to the point below the notch of the protocristid.

The lower molars are slightly worn, increasing in size posteriorly. Trigonid of m1 is strongly anteroposteriorly

TABLE 2 Comparative measurements of *Obotherium tongi* and other related taxa. (in mm) (*: approximate value; #: measured from the plate).

	Obotherium tongi	*Tapirulus perrierensis*	*Tapirulus hyracinus*	*Hexacodus pelodes*	*Microsus cuspidatus*	*Homacodon vagans*
	V 31731	Sudre (1978)		Gazin (1952)	West (1984)	
p1 L	2.50*					
p W	1.30*					
p2 L	3.80*		7			
p2 W	1.50*		2.5			
p3 L	4.72	6	7.2			
p3 W	1.80	2	2.8			
p4 L	5.00	5	6.5	4.5	4.15	5.23
AW/PW	2.85/2.10	2.5	3–3.6	2.8	2.35/2.78	2.77
m1 L	5.21	5–5.3	6–6.6	4.2	4.28	5.25
AW/PW	3.00/3.30	2.8–3	3.1–4.4	3.0	2.5/2.78	3.48/3.88
m2 L	5.43	5.5	6.2–7.1	4.4	4.3	5.40
AW/PW	3.41/3.78	3.2	3.6–4.2	3.7	2.9/3.2	4.0/4.27
m3 L	6.80	6.3–7.5	6.5–7.4	4.75#	5.05	6.77
AW/PW	3.41/3.40	2.8–3	3.2–4.1	2.63#/2.75#	3.03/2.95	4.0/3.7
p1–4 L	15.78		27.1#			
m1–3 L	16.66		21.5#			

compressed with the metaconid lingual to the protoconid. The protoconid and hypoconid are lower than the metaconid and entoconid, respectively. Both protocristid and paracristid are moderately notched and join the apex of the metaconid. The paracristid forms an angled arch anteriorly, while the protocristid is nearly transversely extended. The paraconid is absent. The talonid is considerably wider, longer, and slightly lower than the trigonid. The hypoconid is more buccally placed than the protoconid, extending a cristid obliqua anterolingually to the half height of the protocristid and to the midpoint (or slightly buccal to the notch) of the protocristid. A worn facet is present on the anterobuccal side of the hypoconid. The entoconid is more anteriorly placed than the hypoconid. The hypolophid is complete, widely notched, and slightly anterolingually oblique. The medially placed hypoconulid is well-developed but heavily worn, joining the midpoint of the hypolophid by a long prehypoconulid cristid. The hypoconulid forms a relatively large third lobe with a somewhat pointed posterior border. A narrow worn facet is present along the posterobuccal border of the hypoconulid. The precingulid is distinct, while the cingulids are absent on other sides of the crown.

The m2 is morphologically similar to m1, but the metaconid and entoconid are slightly more anteriorly placed relative to their opposite cuspids than in m1. Furthermore, the hypoconulid joins the hypolophid slightly buccal to the midpoint, and the posterior border of the crown is more rounded. The m1 is placed slightly buccal to the m2, and the hypoconulid of m1 is situated anterior to the protoconid of m2. The morphology of m3 differs from that of m1-2, having a paracristid interrupted at the notch, a talonid slightly wider than the trigonid, a weaker hypolophid with a more isolated entoconid and a bunodont hypoconid, and the entoconid nearly lingual to the hypoconid. The hypoconulid of m3 expands into a large lobe with a prehypoconulid cristid joining the posterolingual side of the hypoconid.

3.8 Comparisons

The lower molars of *Obotherium tongi* share the following characters with *O. parvum*: an anteroposteriorly compressed trigonid, a well-developed hypolophid, an entoconid slightly anteriorly situated to the hypoconid, a distinct, nearly medial-placed hypoconulid on m1-2, a talonid wider than a trigonid on m1-2, a cristid obliqua extending slightly buccal to the midpoint of the protocristid, and a large hypoconulid lobe on m3. The lower molars of *Obotherium tongi* are more advanced than those of *O. parvum* in having a more compressed trigonid without a paraconid, a more complete hypolophid with a long prehypoconulid cristid joining the middle of the hypolophid on m1-2 or directed to the lingual side of the hypoconid on m3, and a more posteriorly extended hypoconulid on m1-2. *Obotherium parvum* and *O. tongi* are clearly closely related, and the latter provides morphologic information about *Obotherium* unknown in *O. parvum*.

The lower jaw of *Obotherium tongi* is characterized by the convex ventral border and concave alveolar border, more similar to the arctocyonid *Chriacus* than to *Diacodexis* (Rose, 1996). The horizontal ramus of the lower jaw in *Diacodexis* is slender and shallow with a nearly straight ventral border, and becomes slightly shallower forwards (Boivin et al., 2018). A fragmentary lower jaw of *Diacodexis indicus* (GU 1622) with a convex ventral border and consistent height between m3 and m1 is unlike other specimens of the same species (Kumar et al. (2010), the differences attributed to sexual dimorphism. Short diastemata are usually present among the teeth from the canine to p3 in *Diacodexis* (Kumar et al., 2010; Boivin et al., 2018), while the premolars and canine of *Obotherium tongi* are closely spaced without diastemata. The shallow lower jaw of *Homacodon* has a less convex ventral border and nearly straight alveolar border compared to *Obotherium tongi* (West, 1984), while lower jaws of other homacodontids, such as *Hylomeryx*, *Mytonomeryx*, and *Pentacemylus*, have a deeper horizontal ramus that shallows anteriorly with nearly straight ventral and alveolar borders (Peterson, 1919; Gazin, 1955). Lower premolars and canine are closely spaced without diastemata in *Homacodon,* the paratype of *Hylomeryx annectens* (CM 2944), and in *Obotherium tongi* (Peterson, 1919; West, 1984). Diastemata are variably present among lower premolars and canine in *Bunomeryx elegans*, *Mytonomeryx*, and *Pentacemylus* (Peterson, 1919; Gazin, 1955). Similarly, the lower jaws of dichobunines (i.e., *Dichobune leporine*), hyperdichobunines (i.e., *Mouillacitherium elegans*), and eurodexeines (i.e., *Eurodexis ceciliensis*, *Parahexacodus germanicus*) can be distinguished from *Obotherium tongi* by the straight or slightly convex ventral border, a straight alveolar border, and diastemata variably present among premolars and canine (Sudre, 1978; Erfurt and Sudre, 1996).

Relatively complete lower jaws of *Tapirulus* are only known from *T. schlosseri* and *T. hyracinus* (Stehlin, 1910). They differ from *Obotherium tongi* in having a straight ventral border and alveolar border, and horizonal ramus becoming shallower forwards. The canine and the premolars are also spaced closely together in *T. schlosseri* (Stehlin, 1910, fig. 216), while short diastemata are present among premolars in *T. hyracinus* (Stehlin, 1910, fig. 217).

The well-developed metaconid on p4 in *Obotherium tongi* is similar to Uintan homacondontids, while the metaconid is absent or incipient in *Hexacodus* and *Homacodon*, and relatively smaller in *Microsus* (Sinclair, 1914; Gazin, 1955). The p4 of dichobunids usually also has a distinct metaconid as in *Obotherium tongi* (Theodor et al., 2007). The p4 of *Tapirulus* (excluding *T. majori,* whose p4 is not preserved) has a distinct metaconid, but p3 of *T. schlosseri*, *T. perrierensis*, and *T. hyracinus* have a much more distinct paraconid and a well-developed cuspid posterior to the protoconid (Stehlin, 1910; Sudre, 1978). The premolar series is elongated and relatively longer than the molar series in later *Tapirulus*, such as *T. schlosseri* and *perrierensis* (Table 2), whereas the premolar series is slightly shorter than the molar series in *O. tongi*.

The convex ventral border and alveolar border of the lower jaw in *Obotherium tongi* are different from those of early artiodactyls, but show some similarities with the arctocyonid *Chriacus* and ruminant *Archaeomeryx* (Vislobokova, 2002). The closely spaced premolars and canine, and distinct metaconid on p4 in *Tapirulus* also support a close phylogenetic relationship with *Obotherium*.

Obotherium aff. *O. tongi*
(Figure 6; Table 1)

Material—IVPP V 31732.1–2 (Figures 6A, D), a left lower jaw with m1 talonid and m2–3, and a left astragalus, the Ulan Shireh Formation, North Mesa; IVPP V 31733 (Figure 6B), a right lower jaw with m3, the Irdin Manha Formation, Huheboerhe (field no. 13069); IVPP V 31734 (Figure 6C), a left lower jaw with m3, the Irdin Manha Formation, Huheboerhe (field no. HIL 174).

3.9 Description

The lower molars of V 31732.1 from Ulan Shireh are similar to those of *O. tongi* in morphology, but the former has a smaller size, a more erect trigonid, a more complete hypolophid, a more reduced hypoconulid on m1–2 with a weak prehypoconulid cristid, a more pointed hypoconulid on m2, and the prehypoconulid cristid of m2-3 joining the midpoint of the hypolophid as in m1. The ventral border of the horizontal ramus is nearly straight. The lower jaw with m1-3 shows some more derived characters than that of *O. tongi*, but due to the lack of more complete material and information about dental variation in *O. tongi*, we tentatively assign the lower jaw to *Obotherium* aff. *O. tongi* instead of a new species of *Obotherium.*

Two lower jaws with left and right m3 from the Irdin Manha Formation at Huheboerhe are assigned to *Obotherium* aff. *O. tongi*. They are similar to V 31732.1 in having a small size, a more complete hypolophid, a prehypoconulid cristid joining the midpoint of the hypolophid, and the hypoconulid lobe relatively small.

A left astragalus (IVPP V 31732.2) is presumed, being found close by IVPP V 31732.1, and represents the same species (Figure 6D). The proximal and distal trochleae are somewhat laterally inclined, and not aligned. The long axis of the proximal trochlea is oriented laterally about 9° (trochlear angle) relative to that of the entire bone, while the long axis of the distal trochlea is oriented medially at the angle of 15°. The proximal trochlea is deep and asymmetrical with the lateral part wider than the medial one. The medial and lateral edges of the trochlear are relatively sharp and roughly equal in height. A relatively wide fossa with a deep pit is present distal to the proximal trochlea for the anterior process of the tibia. The medial surface of the proximal trochlea is nearly vertical with an indistinct shallow fossa on its distal half. A relatively distinct medial process is present posterior to the medial surface of the proximal trochlea. The neck of the astragalus is short but prominent, and is demarcated by a lateral notch. The distal trochlea is divided by a distinct ridge into a wide, shallowly-grooved medial surface for the navicular and a narrow, lateral facet for the cuboid. Proximal to the distal trochlea there is a shallow fossa for the navicular stop. Both the navicular and cuboid facets extend to the posterior side at the same extent, but the cuboid facet tapers towards the posterior side. On the posterior side, the sustentacular facet is convex proximodistally, flat laterally, and elongated rectangular in outline with the long axis parallel to that of the entire bone. The notch between the sustentacular facet and the distal trochlea is relatively shallow. The medial border of the sustentacular facet is limited by an indistinct ridge, which is laterodistally oriented joining the lateral border of the cuboid facet. Lateral to the ridge is a narrow facet which is possibly for the medial sustentacular facet of the calcaneus.

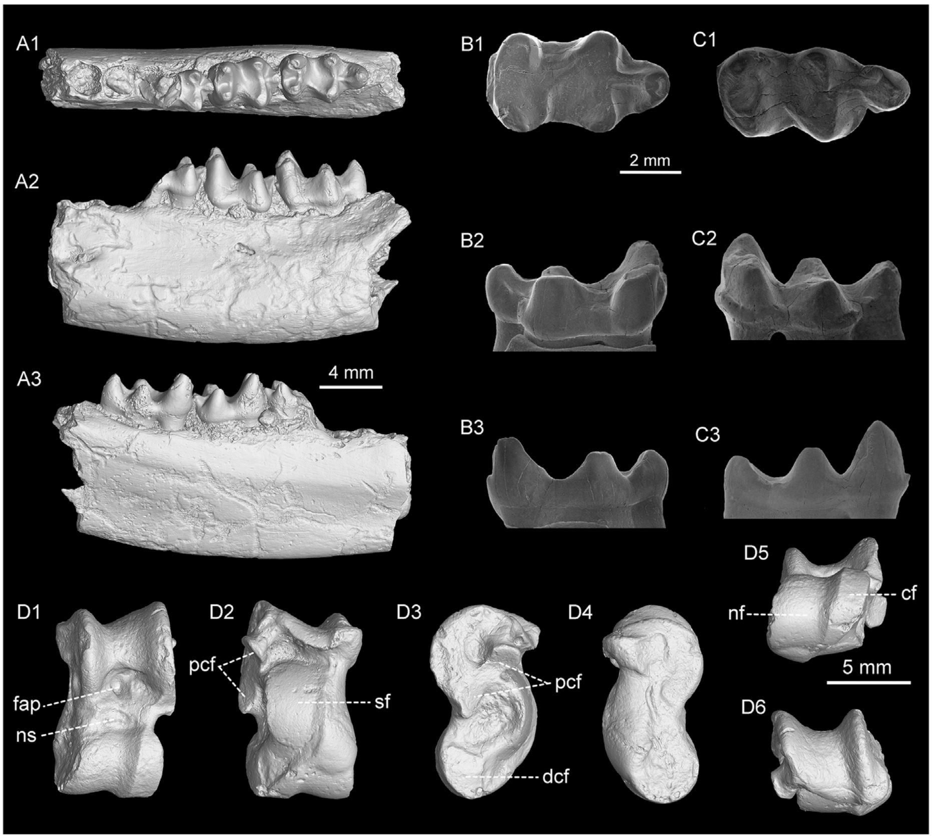

FIGURE 6
Lower jaw, astragalus, and isolated m3 of *Obotherium* aff. *O. tongi* . **(A)** left lower jaw with m1 talonid and m2-3 (IVPP V 31732.1); **(B)** right m3 (IVPP V 31733); **(C)** left m3 (V 31734): **(A1–C1)**, occlusal view; **(A2–C2)**, buccal view; **(A3–C3)**, lingual view; **(D)** left astragalus (IVPP V 31732.2) in **(D1)** anterior; **(D2)** posterior; **(D3)** lateral; **(D4)** medial; **(D5)** distal; and **(D6)** proximal views. Abbreviations: *cf*, cuboid facet; *dcf*, distal calcaneal facet; *fap*, fossa for anterior process of tibia; *nf*, navicular facet; *ns*, fossa serving as a navicular stop; *pcf*, proximal calcaneal facet; *sf*, sustentacular facet.

Medial to this ridge there is a slightly inflated surface, which becomes wider distally, for the plantar calcaneonavicular ligament. The proximal calcaneal facet on the lateral side of the astragalus is narrow, elongated, and concave, facing more laterally than posteriorly. The astragalar sulcus is relatively distinct on the posterior side, separating the sustentacular facet from the proximal calcaneal facet. On the lateral side, there is a wide and relatively shallow fossa between the two facets. A small, shallow fossa on the lateral surface of the proximal trochlea is present above the proximal calcaneal facet. The distal calcaneal facet is relatively large, fan-shaped, and flat.

Astragalar Measurements (IVPP V 31732.2, in mm): Length=11.87; Trochlear width=5.79; Distal width=5.53; Navicular width=4.02.

3.10 Comparisons

Vislobokova (2004a) erected a new species *Chorlakkia valerii* for a left lower jaw with m2–3 from the middle Eocene of Khaichin-Ula II, Mongolia. As noted by Vislobokova (2004a), *Chorlakkia valerii* is distinguished from the type species *Chorlakkia hassani* by the absence of twinned entoconid and hypoconulid on the lower molars (Gingerich et al., 1979), and by possession of other advanced characters, such as relatively elongated crowns of m2 and m3, a wider talonid compared to the trigonid, a more anterior position of the entoconid, and a narrower hypoconulid of m3. We suggest *Chorlakkia valerii* is better assigned to *Obotherium* based on an anteroposteriorly compressed trigonid, a talonid wider than the trigonid, an entoconid more anteriorly placed to the hypoconid, a cristid obliqua extending buccally to the midpoint of the protocristid, a well-developed hypoconulid in medial position, a transversely extended posthypocristid, and a possibly weak hypolophid according to the plate 9 of Vislobokova (2004a). The combination of a posthypocristid transversely extending to the midpoint of the crown on m3, a relatively small hypoconulid on m3, an erect trigonid and the lack of the paraconid in *Obotherium valerii* (=‘*Chorlakkia*’ *valerii*) indicate it is more similar to *O. tongi* than to *O. parvum*.

The astragali of *Diacodexis*, *Eurodexis*, and *Elaschitotherium* are compared with that of *Obotherium* (Guthrie, 1968; West, 1984; Martinez and Sudre, 1995; Sudre and Erfurt, 1996; Métais et al., 2004; Kumar et al., 2010). The astragalus of *Obotherium* generally resembles *Diacodexis* and *Eurodexis* in having a distal trochlea medially deflected to the proximal trochlea, a distinct ridge separating the navicular and cuboid facets on the distal trochlea, and a well-developed facet for the plantar calcaneonavicular ligament. The astragalus of *Obotherium* is

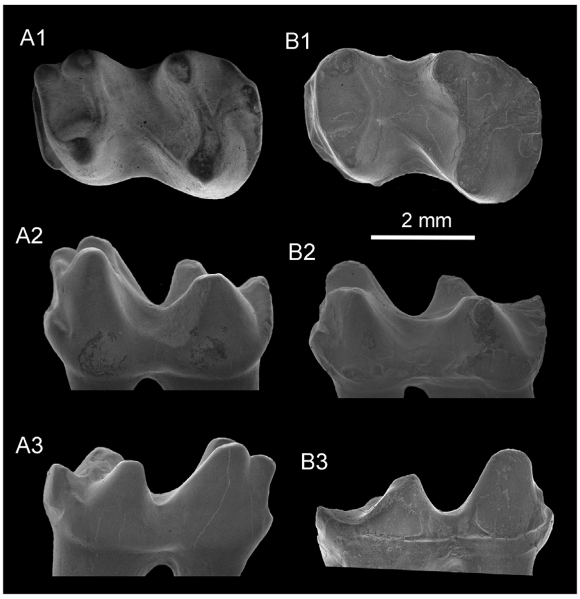

FIGURE 7
The lower molars of *Obotherium* sp.1 **(A)** and *Obotherium* sp. 2 **(B)**. **(A)** left m1/2 (IVPP V 31735); **(B)** left m1/2 (V 31736): **(A1–B1)**, occlusal view; **(A2–B2)**, buccal view; **(A3–B3)**, lingual view.

more similar to *Diacodexis indicus* than to *Eurodexis* and North American *Diacodexis* in having a deep fossa for the anterior process of tibia, and the navicular and cuboid facet equally extended towards the posterior side (Schaeffer, 1947; Martinez and Sudre, 1995; Sudre and Erfurt, 1996; Kumar et al., 2010). The astragalus of *Elaschitotherium*, which resembles that of *Eurodexis*, is distinguished from *Obotherium* by a shallow fossa for the anterior process of the tibia, a less distinct ridge separating the navicular and cuboid facets, navicular facet more posteriorly extended than the cuboid facet, and two separated proximal calcaneal facets (Métais et al., 2004).

Obotherium sp. 1
(Figure 7A; Table 1)

Material—IVPP V 31735, a left m1/2 from the Irdin Manha Formation at Huheboerhe (field no. 13088).

3.11 Description

The left m1/2 differs from both *Obotherium tongi* and *O. parvum* in having a relatively longer trigonid with a more distinct and separate paraconid. The complete hypolophid and distinct hypoconulid with a long prehypoconulid cristid are similar to those of *O. tongi*.

Obotherium sp. 2
(Figure 7B; Table 1)
Material—IVPP V 31736, a left m1/2 from the Irdin Manha Formation at Irdin Manha (field no. 11377).

3.12 Description

The m1/2 is similar to *Obotherium tongi* in having an anteroposteriorly compressed trigonid, a complete hypolophid, and a posteriorly pointed hypoconulid with a long prehypoconulid cristid. But the prehypoconulid cristid is more oriented to the hypoconid in IVPP V 31736 than in *O. tongi*. The m1/2 probably represents a variation of *O. tongi*.

Tapiruloides gen. nov.
Type species—*Tapiruloides usuensis* gen. et sp. nov.
Etymology—Greek, -*oides*, like; in allusion to its similarities with *Tapirulus*.
Included species—type species only.
Diagnosis—Lower molars nearly bilophodont; trigonid highly anteroposteriorly compressed without a paraconid, talonid wider than trigonid with entoconid more anteriorly placed than hypoconid, complete hypolophid slightly notched, cristid obliqua almost absent, prehypoconulid cristid joining the midpoint of the hypolophid in a high position, and hypoconulid of m3 high and beak-like.
Differential diagnosis—Differs from *Tapirulus* and *Obotherium* by almost absent cristid obliqua on the lower molars and a beak-like hypoconulid on m3; further differs from *Tapirulus* by a slightly more anteriorly placed entoconid to the hypoconid on the lower molars.
Age and Distribution—Sharamurunian (middle Eocene) of the Erlian Basin, Inner Mongolia, China.

Tapiruloides usuensis gen. et sp. nov.
(Figure 8; Table 1)
Holotype—IVPP V 31737, a left lower jaw with m2-3.
Etymology—In reference to the locality of the holotype “Ula Usu”, meaning “the well of mountain water” in Mongolian.
Diagnosis—as for the genus.
Locality and horizon—the base of the Shara Murun Formation, Ula Usu (field no. 10013), Erlian Basin.

3.13 Description

The horizontal ramus below m2–3 is shallow and slightly convex. The preserved anteroventral portion of the masseteric fossa is relatively deep.

The metaconid, entoconid, and hypoconulid of m2 are partially broken. The m2 is bilophodont. The trigonid is strongly anteroposteriorly compressed without a paraconid. The high paracristid and protocristid connect the protoconid and metaconid anteriorly and posteriorly, respectively. The protocristid is slightly deeper notched. The talonid is longer and wider than the trigonid. The hypolophid, which is composed of transverse posthypocristid and postentocristid, is high and nearly complete with a shallow notch between the junction. The entoconid is slightly more anteriorly placed than the hypoconid. A small, oval-shaped worn facet is obliquely aligned at the base of the talonid between the protocristid and hypolophid, representing the vestige of the cristid obliqua. Although the hypoconulid is partially broken, it is relatively large and posteriorly extended. The anterior extremity of the

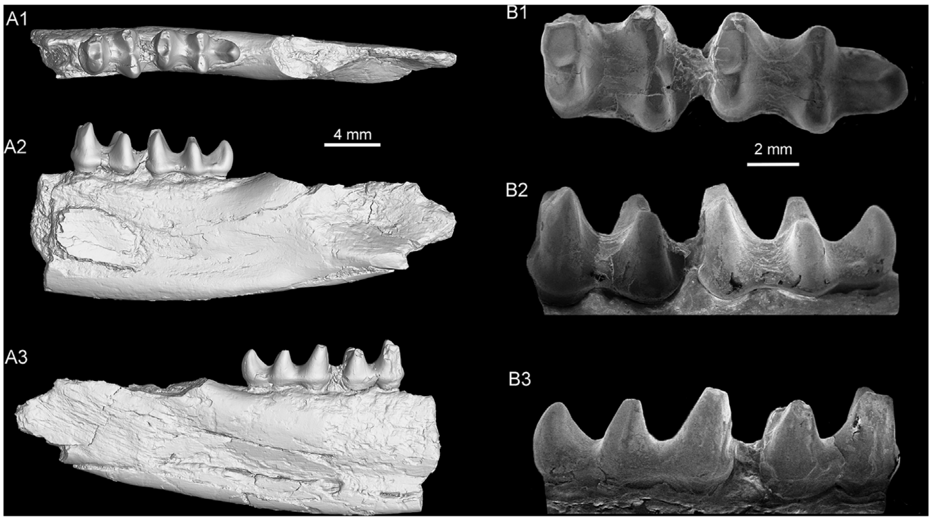

FIGURE 8
Left lower jaw of *Tapiruloides usuensis* gen. et sp. nov. with m2-3 (IVPP V 31737). **(A1–B1)** occlusal view; **(A2–B2)**, buccal view; **(A3–B3)**, lingual view.

prehypoconulid cristid joins the hypolophid in a high position that is slightly below the notch of the latter. A weak but distinct precingulid is present.

The m3 is similar to m2 in morphology, but the former has a talonid slightly wider than the trigonid, and the entoconid is nearly lingually placed to the hypoconid. Furthermore, the hypoconulid of m3 is expanded into a third lobe, and the apex of the hypoconulid is beak-like, as high as the hypoconid. The prehypoconulid cristid is sharp and straight, descending from the hypoconulid to the posterior side of the hypolophid, where a weak ridge rises again to a relatively high position below the notch of the hypolophid. The prehypoconulid cristid divides the hypoconulid lobe into two equal-sized, steep lingual and buccal surfaces. A tiny cingulid is present at the base of the buccal side of the hypoconulid lobe.

3.14 Comparisons

The species probably derived from *Obotherium* based on the following synapomorphies on m2–3: Anteroposteriorly compressed trigonid, talonid wider than the trigonid, a slightly anteriorly placed entoconid to the hypoconid, and a well-developed hypoconulid. The m2-3 of V 31737 shows some more derived characters than *Obotherium* in having a more complete hypolophid, nearly vertical trigonid, and a nearly absent cristid obliqua. On the other hand, V 31737 strikingly resembles *Tapirulus perrierensis* and *T. hyracinus* in having bilophodont dentitions (Stehlin, 1910; Sudre, 1978), but differs from the latter two species by a talonid wider than the trigonid, a relatively short talonid on m2, and a nearly absent cristid obliqua. The assignment of the specimen to a new genus rather than to *Tapirulus* is based not only on the morphologic differences but also on the observation that V 31737 is probably more closely related to *Obotherium* than to *Tapirulus*.

4 Discussion

4.1 Phylogenetic position of *Obotherium* and *Tapiruloides*

In order to investigate the phylogenetic position of *Obotherium* within early artiodactyls, a cladistic analysis was conducted based on the morphological data matrix modified from Métais et al. (2004). The data matrix of Métais et al. (2004), comprising 26 dental characters and 26 taxa, includes early artiodactyl groups from Eurasia and North America, such as Homacodontidae and Lantianiinae. Five taxa (*Obotherium parvum*, *O. tongi*, *Tapiruloides usuensis*, *Tapirulus majori*, and *T. hyracinus*) and eight characters were added to the Métais et al. (2004) matrix, with modifications of four original character states (character 14–16, 18). The character states of the upper molar in *Obotherium parvum* were based on the specimen IVPP V 31730 assigned to ? *O. parvum*, and the character states of the lower molar in *Eolantianus* were changed to the question marks due to doubtful association with upper teeth. The modified data matrix is comprised of 31 taxa with three outgroups and 34 dental characters (Supplementary Material). The cladistic analyses result in 124 MPTs, each with 163 steps. Both a strict consensus tree (CI = 0.343, RI = 0.626) and a 50% majority-rule consensus tree (CI = 0.277, RI = 0.490) were constructed (Figure 9).

Although many polytomies are present in the topology of the strict consensus tree (Figure 9A), several clades are supported. *Obotherium*, *Tapiruloides*, and *Tapirulus* form a polytomous clade, which is nested in a polytomy with homacodontids, *Dichobune*, *Cuisitherium*, and a 'ruminant' clade. This polytomy group forms a sister group to *Hyperdichobune*-Lantianiinae, and Lantianiinae is composed of *Eolantianus* as a sister group to a *Lantianus*-*Elaschitotherium* clade. *Eurodexis*, *Pakibune*, *Chorlakkia*, and *Diacodexis* are polytomous basal groups. The *Obotherium*-*Tapirulus*-*Tapiruloides* clade is supported by seven unambiguous

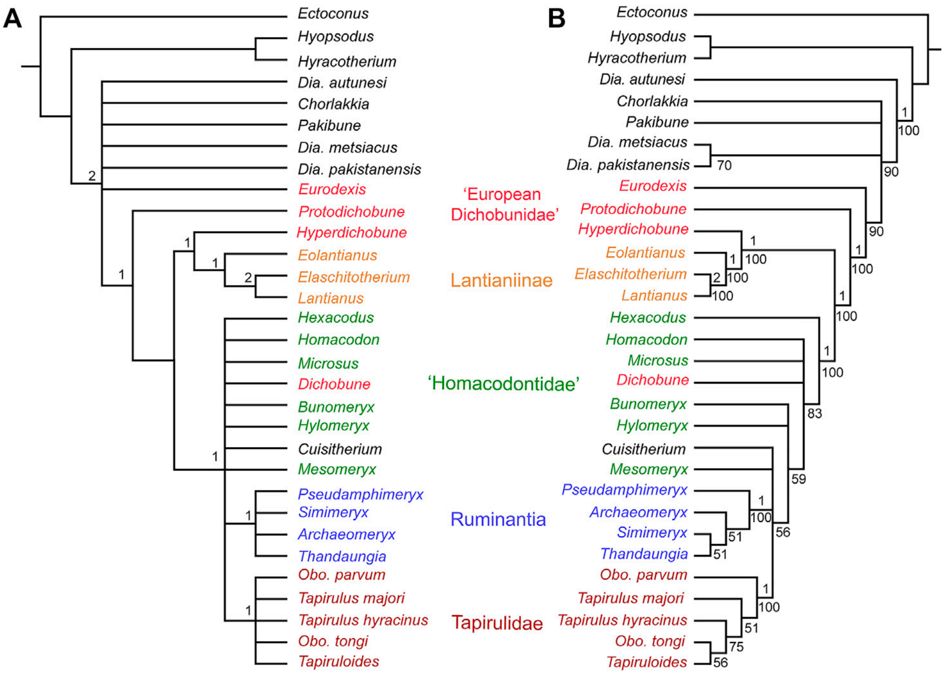

FIGURE 9
Strict consensus **(A)** and 50% majority-rule consensus **(B)** trees of the 124 MPTs in the phylogenetic analyses of the early artiodactyls with a focus on Tapirulidae. Values above the branches are Bremer Support at the nodes, and below the branches are the percentage of 50% majority-rule consensus trees.

synapomorphies: developed premetaconule cristae on the upper molars (8:1→2), continuous lingual cingulum (12:1→0), absent buccal cingulids on the lower molars (14:1→2), well-developed p4 metaconid (25:1→2), strong p4 paraconid (26:1→2), transversely extended posthypocristid (32:1→2), and a long m1-2 hypoconulid (33:0→1). Thus, the enigmatic European *Tapirulus* is not a choeropotamid, a tylopod, an anoplotheriid, or a dacrytheriid (Hooker and Thomas, 2001; Erfurt and Métais, 2007), but is closely related to *Obotherium* and *Tapiruloides* from Asia. The Tapirulidae were probably descended from a North American basal homacodontid, such as *Hexacodus* from the middle and late Wasatchian. Although Métais et al. (2004) noticed striking resemblances between primitive European hyperdichobunines and Asian lantianiines, they attributed the similarities to convergence. However, our topology shows the two subfamilies from a sister group, supported by well-developed parastyles on the upper molars (13:1→2).

The 50% majority-rule consensus tree partially resolves some of these polytomies (Figure 9B). *Tapiruloides* and *Obotherium tongi* are sister taxa, and *Tapirulus hyracinus*, *Tapirulus majori*, and *Obotherium parvum* are successive sister taxa to the *Tapiruloides-Obotherium tongi* clade. The result implies that *Obotherium parvum* is the most basal taxon within the clade, and both *Obotherium* and *Tapirulus* are paraphyletic. Paraphyly of *Obotherium* could be attributed to the lack of upper dentition in *Tapiruloides* and *Obotherium tongi*. *Pseudamphimeryx* is included within Ruminantia as a sister group to *Archaeomeryx* and *Simimeryx-Thandaungia* clade. Ruminantia is supported by gradual increase in size from M1 to M2 (1:1→3), buccal cingulum absent on the upper molars (4:1→0), postprotocrista and metaconule connection present (6:0→1), and postcingulid weak (24:1→0). The European endemic Amphimerycidae including *Amphimeryx* and *Pseudamphimeryx* was considered to be more closely related to xiphodontids or dacrytheriids than to ruminants, although a fused cubonavicular is present in *Amphimeryx collatarsus* (Erfurt and Métais, 2007). Similarly, Amphimerycidae is a sister group to *Archaeomeryx* within European bunoselenodont families (Luccisano et al., 2020), suggesting it is allied with ruminants (Simpson, 1945; McKenna and Bell, 1997). *Cuisitherium* is controversial, having been assigned to Dacrytheriidae (Sudre et al., 1983), Choeropotamidae (Hooker and Thomas, 2001; Erfurt and Métais, 2007), or Haplobunodontidae (Luccisano et al., 2020). Our analyses indicate that *Cuisitherium* is probably allied with ruminants and tapirulids. Homacodontidae is not monophyletic, and *Hexacodus* represents the most basal taxon consistent with its primitive characters and early Eocene age. It is interesting that *Dichobune* is more closely related to homacodontids than to other European endemic artiodactyls, consistent with the topology of basal artiodactyls by Luccisano et al. (2020). *Protodichobune* and *Eurodexis* are successive sister groups to Lantianiinae-Hyperdichobuninae and Homacodontidae-*Dichobune-Cuisitherium*-Ruminantia-Tapirulidae clade. *Diacodexis* is not monophyletic, and *D. antunesi* is a sister group to other early artiodactyls in this analysis; but *Diacodexis* is monophyletic in the Luccisano et al. (2020)

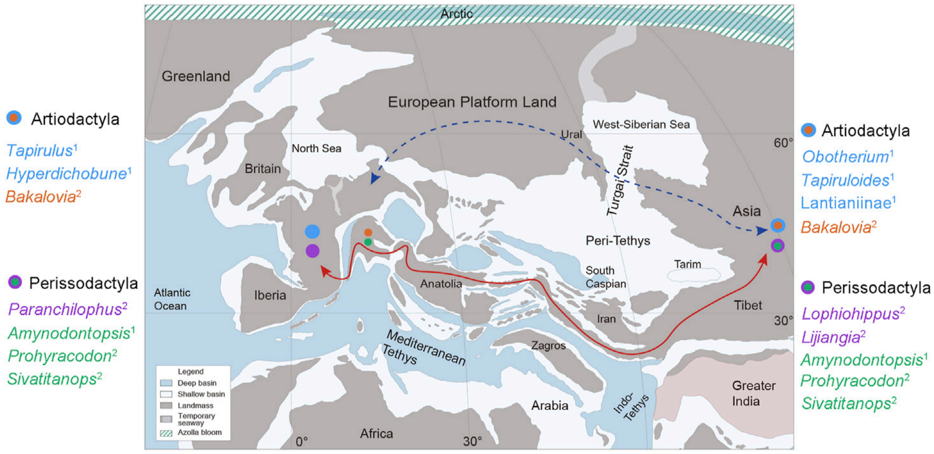

FIGURE 10
Paleogeography of Tethys region during the middle Eocene and probable dispersal routines between Asian and European mammal groups. The superscript numbers 1 and 2 indicate the early middle Eocene and late middle Eocene taxa, respectively. (The paleogeographic map was modified from Palcu and Krijgsman, 2022, fig. 8, with permission from W. Krijgsman).

phylogeny. *Pakibune* and *Chorlakkia* are unresolved basal groups of early artiodactyls.

4.2 Palaeobiogeography

Europe was connected with North America and Asia during the early Eocene (McKenna, 1975; 1983; Krause and Maas, 1990); however, after the Early Eocene, Europe, mainly composed of archipelagos, was isolated from Asia and North America until the Oligocene. The European mammalian faunas from the middle through late Eocene are mostly endemic. By contrast, immigration of mammals was frequent between Asia and North America *via* the Bering land bridge during the middle and late Eocene (Woodburne, 2004), and Eocene mammals from Asia show more or less similarity with those from North America, but share few taxa with Europe.

Erfurt and Métais (2007) noted that the Geiseltalian/Robiacian transition (MP13/14) is characterized by the sudden appearance of several selenodont artiodactyls in Europe, however, the origin of these endemic selenodont artiodactyls remains obscure. Heissig (1993) proposed a close relationship between anoplotheriids and North American oreodonts based on astragalar morphology, and they may have dispersed from eastern Europe "Fennosarmatian Platform", which was separated from western Europe during the middle and late Eocene by broad seaways from the North Sea Basin to the Black Sea. The European endemic Mixtotheriidae, Cainotheriidae, Anoplotheriidae, and Xiphodontidae have been included in Tylopoda (Gentry and Hooker, 1988; Theodor et al., 2005), and their first appearances are at MP13 or MP14 (Erfurt and Métais, 2007). Amphimerycidae has long been included in Ruminantia (McKenna and Bell, 1997; Theodor et al., 2005), but their similarities are attributed to convergence (Métais et al., 2004). Erfurt and Métais (2007) suggest these endemic artiodactyls are of autochthonous origin from unknown European dichobunoids. However, our analyses show *Obotherium* and *Tapiruloides* are closely related to *Tapirulus*, and *Obotherium parvum* is the most basal taxon in the clade and probably gave rise to European *Tapirulus*. Morphological similarities between Irdinmanhan *Obotherium* and *T. majori*, *T. depereti* from MP13 and MP14 suggest a biogeographic connection between Asia and Europe during the early middle Eocene. Thus, some endemic European artiodactyls are probably of allochthonous origin from Asia as exemplified by *Obotherium* and *Tapirulus*. In addition, the earliest *Hyperdichobune* from MP13 and Asian Lantianiinae are also closely related, supporting a connection between Europe and Asia during the early middle Eocene. Dispersal routes between Europe and Asia during the middle-late Eocene are across the Turgai Strait or more likely along the Tethyan shore as evidenced by shared perissodactyls and other mammal groups (Figure 10) (Böhme et al., 2013; Missiaen and Gingerich, 2014; Bai, 2017; Palcu and Krijgsman, 2022). The Balkanatolia mammalian fauna from the Balkans to the Caucasus is characterized by an endemic phase during the Ypresian and Lutetian, and an invasive phase from Asian taxa during the Bartonian-Priabonian (Licht et al., 2022). Although many Asian ungulates and rodents first appeared during the late middle Eocene (Bartonian) in Balkanatolia, the first appearance of Asian-derived *Amynodontopsis* aff. *bodei* (Tissier et al., 2018; Licht et al., 2022) and western Europe derived *Galatiadelphys* (Métais et al., 2018) from the upper Lutetian suggests that a possible southern route emerged and facilitated the dispersal during the early middle Eocene.

The nearly contemporary North American artiodactyl assemblage is characterized by the first appearance of agriochoerids, oromerycids, and protoceratids in the middle Uintan (Ui2), and the first appearance of hypertragulids, leptomerycids, and anthracotheriids in the late Uintan (Ui3) (Janis et al., 1998; Erfurt and Métais, 2007). These new forms may be derived North American homacodontids (Stucky, 1998) or immigrants from Asia (Vislobokova, 1998; Métais and Vislobokova, 2007). The latter hypothesis needs further investigation and fieldwork on Eocene artiodactyls from Asia. The Irdinmanhan ALMA, which is usually correlated with the Uintan NALMA (Bai et al., 2017; Speijer et al., 2020; Bai et al., 2021), could be at least correlated to European MP13-14 based on the similarities between *Obotherium* and early *Tapirulus*.

4.3 Evolution of bilophodont teeth in artiodactyls

The teeth of artiodactyls are divided into bunodont and selenodont types, as well as the intermediate bunoselenodont. Both selenodonty in ruminants and bilophodonty in tapirulids probably derived from the bunoselenodont early homacodontid *Hexacodus*. From the Irdinmanhan *Obotherium* to Sharamurunian *Tapiruloides*, the main changes in the lower molars lie in the reduction of the paraconid and cristid obliqua, a more complete hypolophid, and elongated hypoconulid on m1-2. The relatively long prehypoconulid cristid in *Obotherium tongi* is likely derived from a posterolingually extended branch of the bifurcated posthypocristid in *O. parvum*. The prehypoconulid cristid joins the point buccal to the midpoint of the hypolophid on m1-2 in *Obotherium parvum*, but it nearly joins the midpoint of hypolophid in *O. tongi* and *Tapiruloides*. Bilophodont teeth are completely formed in *Tapiruloides*, but the trigonid still retains a narrow redundant basin. Similarly, the lower molars of *Tapirulus hyracinus* and *T. perrierensis* are essentially bilophodont with a reduced cristid obliqua and a narrow trigonid basin (Sudre, 1978). The evolution of bilophodont upper molars in *Tapirulus* lies in the compression and elevation of the protoloph and crescentic metaconule, reduction of the paraconule, and strongly buccally deflected centrocrista (Sudre, 1978). Stehlin (1910) suggested that the "posterior loph" joining the lingual side of the metacone on the upper molars in *Tapirulus schlosseri* developed from a median crista (endometacristule) between the crescentic metaconule in *T. depereti*, so the "metaloph" in later *Tapirulus* is not homologous with the premetaconule crista as in most artiodactyls. More complete material of the upper molars of early *Tapirulus* is required to verify this explanation.

Raoellidae is an endemic artiodactyl group known from the early to middle Eocene deposits in the Indo-Pakistani subcontinent, characterized by bilophodont upper molars (Thewissen et al., 1987; Theodor et al., 2007; Singh Rana et al., 2021). Orliac and Ducrocq (2012) assigned m3 and p4, originally included in indeterminate Suiodea (Métais et al., 2008), from the Shanghuang fissure of China to raoellid ?*Khirtharia* cf. *major*. The bilophodont upper molars of Raoellidae are characterized by weak or small paraconules, and posterior crest contacting the base of the middle of the metacone (Thewissen et al., 1987); thus, Thewissen et al. (1987) suggest that Raoellidae may be related to *Tapirulus*. But the upper molars of Raoellidae have a more or less straight centrocrista in contrast to the W-shaped ectoloph in derived *Tapirulus*. It is controversial whether the posterolingual cusp on the upper molars in Raoellidae is a metaconule or hypocone (Theodor et al., 2007; Thewissen et al., 2020). The lower molars of Raoellidae have a distinct cristid obliqua, and lack the hypoconulids on m1-2 (Thewissen et al., 1987), while those of *Tapirulus* usually have reduced or absent cristid obliqua and well-developed hypoconulids on m1-2 (Sudre, 1978). The similar bilophodont upper molars in Raoellidae and *Tapirulus* is therefore attributed to the convergence. Raoellidae has recently been considered to be the sister to Cetacea (Thewissen et al., 2007; Cooper et al., 2012; Thewissen et al., 2020), and distantly related to *Tapirulus*.

Some listriodontine and schizochoerine suids from the Neogene also developed bilophodont molars, such as the listriodontines *Listriodon*, *Lopholistriodon* and schizochoerines *Yunnanochoerus*, *Schizochoerus* from the Miocene of Eurasia and Africa with lophodont molars, which were derived from bunolophodont groups with accessory cusps (van der Made and Han, 1994; van der Made, 1996; van der Made, 1997; Pickford and Morales, 2003; Harris and Liu, 2007). The multiple appearances of bilophodont teeth in different lineages of artiodactyls are attributed to the convergence and are convergent on the bilophodont teeth in Tapiridae.

Data availability statement

The datasets presented in this study can be found in online repositories. The names of the repository/repositories and accession number(s) can be found in the article/Supplementary Material. The data matrix was deposited in Morphobank (Project 4563).

Author contributions

All authors contributed to the initial discussions. BB, Y-QW, and JM designed the research. BB wrote the manuscript and analyzed data; Y-QW, JT, and JM improved and edited the manuscript; BB prepared the figures; BB and Y-QW collected data.

Funding

Funding was provided by grants from the Strategic Priority Research Program of the Chinese Academy of Sciences (XDB26000000), the National Natural Science Foundation of China (42272011 and 41672014), Frick Funds from the Division of Paleontology, American Museum of Natural History, and a Discovery Grant from the Natural Sciences and Engineering Research Council of Canada.

Acknowledgments

We are grateful to Qian Li, Xun Jin, Fang-Yuan Mao, Hai-Bing Wang, Wei Zhou, Shi-Jie Li, Qi Li, Cheng-Kai Sun, Yong-Xing Wang, Yong-Fu Wang, Xiao-Yang Wang, Ran-Cheng Xu, Hai Xing, Xin-Yue Zhang (all IVPP), K. Christopher Beard (University of Kansas, Lawrence, United States), and Daniel L. Gebo (Northern Illinois University, DeKalb, United States) for assistance in the field; Xun Jin and Wei Gao (both IVPP) for photography; Ye-Mao Hou (IVPP) for μ-CT scanning; Yong Xu for the drawing of Figure 5; Zhao-Qun Zhang, Ban-Yue Wang, Xi-Jun Ni, Jie Ye, Zhan-Xiang Qiu, and Su-Kuan Hou (all IVPP) for helpful discussion. We thank O. Maridet, P. Li, M. Scheuplein, and D. Mertmann for providing important references; A. Henrici and A. McAfee (both Carnegie Museum of Natural History) for taking photos of *Hylomeryx annectens* (CM 2335); S. Fu and W. Krijgsman for the permission of usage of geological map in Figure 1 and paleogeographic map in Figure 9, respectively.

Conflict of interest

The authors declare that the research was conducted in the absence of any commercial or financial relationships that could be construed as a potential conflict of interest.

The handling editor LFF declared a past co-authorship with the author JM.

Publisher's note

Supplementary material

The Supplementary Material for this article can be found online at: https://www.frontiersin.org/articles/10.3389/feart.2023.1117911/full#supplementary-material

References

Averianov, A. O. (1996). Artiodactyla from the early Eocene of Kyrgyzstan. *Palaeovertebrata* 25, 359–369.

Averianov, A. O., and Godinot, M. (2005). Ceratomorphs (mammalia, Perissodactyla) from the early Eocene Andarak 2 locality in Kyrgyzstan. *Geodiversitas* 27, 221–237.

Bai, B. (2017). Eocene pachynolophinae (Perissodactyla, palaeotheriidae) from China, and their palaeobiogeographical implications. *Palaeontology* 60, 837–852. doi:10.1111/pala.12319

Bai, B., Meng, J., Janis, C. M., Zhang, Z. Q., and Wang, Y. Q. (2020). Perissodactyl diversities and responses to climate changes as reflected by dental homogeneity during the Cenozoic in Asia. *Ecol. Evol.* 10, 6333–6355. doi:10.1002/ece3.6363

Bai, B., Wang, Y.-Q., Zhang, X.-Y., and Meng, J. (2021). A new species of the "condylarth" *Hyopsodus* from the middle Eocene of the Erlian Basin, Inner Mongolia, China, and its biostratigraphic implications. *Acta Palaeontol. Pol.* 66, 767–777. doi:10.4202/app.00908.2021

Bai, B., Wang, Y. Q., Li, Q., Wang, H. B., Mao, F. Y., Gong, Y. X., et al. (2018). Biostratigraphy and diversity of Paleogene perissodactyls from the Erlian Basin of Inner Mongolia, China. *Am. Mus. Novit.* 3914, 1–60. doi:10.1206/3914.1

Bai, B., Wang, Y. Q., Mao, F. Y., and Meng, J. (2017). New material of Eocene helaletidae (Perissodactyla, tapiroidea) from the Irdin Manha Formation of the Erlian Basin, inner Mongolia, China and comments on related localities of the Huheboerhe area. *Am. Mus. Novit.* 3878, 1–44. doi:10.1206/3878.1

Böhme, M., Aigstorfer, M., Antoine, P.-O., Appel, E., Havlik, P., Métais, G., et al. (2013). Na duong (northern vietnam) – An exceptional window intoEocene ecosystems from south-east Asia. *Zitteliana* A53, 120–167.

Boivin, M., Orliac, M. J., Antunes, M. T., Godinot, M., Laurent, Y., Marandat, B., et al. (2018). New material of *Diacodexis* (mammalia, artiodactyla) from the early Eocene of southern Europe. *Geobios* 51, 285–306. doi:10.1016/j.geobios.2018.06.003

Brunet, M., and Sudre, J. (1980). Deux nouveaux dichobunides (Artiodactyla, Mammalia) de l'Oligocene inferieur d'Europe. *Proc. Koninklijke Nederl. Akademie van Wetenschappen (B)* 83, 121–143.

Coombs, M. C., and Coombs, W. P. (1977). Dentition of *Gobiohyus* and a reevaluation of the helohyidae (artiodactyla). *J. Mammal.* 58, 291–308. doi:10.2307/1379328

Cooper, L. N., Thewissen, J. G. M., Bajpai, S., and Tiwari, B. N. (2012). Postcranial morphology and locomotion of the Eocene raoellid indohyus (artiodactyla: Mammalia). *Hist. Biol.* 24, 1–32. doi:10.1080/08912963.2011.624184

Ducrocq, S., Soe, A. N., Aung, A. K., Benammi, M., Bo, B., Chaimanee, Y., et al. (2001). A new anthracotheriid artiodactyl from Myanmar, and the relative ages of the Eocene anthropoid primate-bearing localities of Thailand (Krabi) and Myanmar (Pondaung). *J. Vertebrate Paleontology* 20, 755–760. doi:10.1671/0272-4634(2000)020[0755:ANAAFM]2.0.CO;2

Ducrocq, S., Soe, A. N., Chavasseau, O., Sein, C., Chaimanee, Y., Lazzari, V., et al. (2020). New basal ruminants from the Eocene of the pondaung formation, Myanmar. *J. Vertebrate Paleontology* 39, e1722682. doi:10.1080/02724634.2019.1722682

Ducrocq, S., Soe, A. N., Sein, C., Chaimanee, Y., Chavasseau, O., and Jaeger, J.-J. (2022). *Neochorlakkia myaingensis* n. gen., n. sp., a new Dichobunidae (Mammalia, Cetartiodactyla) from the middle Eocene Pondaung Formation, Myanmar. *Comptes Rendus Palevol* 21, 115–122. doi:10.5852/cr-palevol2022v21a4

Ducrocq, S., Soe, A. N., Sein, C., Lazzari, V., Chaimanee, Y., Valentin, X., et al. (2016). First record of a diacodexeid artiodactyl in the middle Eocene Pondaung Formation (Myanmar). *Palaeontol. Z.* 90, 611–618. doi:10.1007/s12542-016-0283-y

Erfurt, J., and Métais, G. (2007). "Endemic European Paleogene artiodactyls," in *The evolution of artiodactyls*. Editors D. R. Prothero and S. E. Foss (Baltimore: John Hopkins University Press), 59–84.

Erfurt, J., and Sudre, J. (1996). Eurodexeinae, eine neue unterfamilie der Artiodactyla (Mammalia) aus dem unter-und mitteleozän europas. *Palaeovertebrata* 25, 371–390.

Franzen, J. L. (1981). Das erste Skelett eines Dichobuniden (Mammalia, Artiodactyla), geborgen aus mitteleozänen Ölschiefem der "Grube Messel" bei Darmstadt (Deutschland, S-Hessen). *Senckellb. Lethaea* 61, 299–353.

Franzen, J. L. (1994). Neue Säugerfunde aus dem Eozän des Eckfelder Maares bei Manderscheid (Eifel). *Mainz. Naturwiss. Arch. Beih.* 16, 177–187.

Fu, S., Liu, Z., Ge, J., Tian, N., Yin, K., Wang, X., et al. (2021). Tectono-sedimentary analysis of the lower cretaceous succession in the sags of the ondor sum uplift, southern Erlian Basin, NE China. *Mar. Petroleum Geol.* 124, 104851. doi:10.1016/j.marpetgeo.2020.104851

Gabunia, L. K. (1971). On a new representative of condylarths (condylarthra) from the Eocene of zaisan depression. *Bull. Acad. Sci. Georgian SSR* 61, 233–235.

Gabunia, L. K. (1973). On the presence of the diacodexinae in the Eocene of Asia. *Bull. Acad. Sci. Georgian SSR* 71, 741–744.

Gazin, C. L. (1962). A further study of the lower Eocene mammalian faunas of southwestern Wyoming. *Smithson. Misc. Collect.* 144, 1–98.

Gazin, C. L. (1955). A review of the upper Eocene artiodactyla of North America. *Smithson. Misc. Collect.* 128, 1–96.

Gazin, C. L. (1952). The lower Eocene Knight Formation of Western Wyoming and its mammalian faunas. *Smithson. Misc. Collect.* 117, 1–82.

Gentry, A., and Hooker, J. (1988). "The phylogeny of the Artiodactyla," in *The phylogeny of the tetrapods*. Editor M. J. Benton (Oxford: Clarendon Press), 235–272.

Gingerich, P., Russell, D. E., Sigogneau-Russell, D., and Hartenberger, J. (1979). "*Chorlakkia hassani*, A new middle Eocene dichobunid (mammalia, artiodactyla) from the kuldana formation of kohat (Pakistan)," in *Contributions from the Museum of Paleontology* (Ann Arbor, Michigan: University of Michigan), 25, 117–124.

Goloboff, P. A., and Catalano, S. A. (2016). TNT version 1.5, including a full implementation of phylogenetic morphometrics. *Cladistics* 32, 221–238. doi:10.1111/cla.12160

Goloboff, P. A., Farris, J. S., and Nixon, K. C. (2008). TNT, a free program for phylogenetic analysis. *Cladistics* 24, 774–786. doi:10.1111/J.1096-0031.2008.00217.X

Guthrie, D. A. (1968). The tarsus of Early Eocene artiodactyls. *J. Mammal.* 49, 297–302. doi:10.2307/1377987

Harris, J. M., and Liu, L. P. (2007). "Superfamily suoidea," in *The evolution of artiodactyls*. Editors D. R. Prothero and S. E. Foss (Baltimore: The Johns Hopkins University Press), 130–150.

Heissig, K. (1993). The astragalus in anoplotheres and oreodonts, phylogenetical and paleogeographical implications. *Kaupia* 3, 173–178.

Hooker, J. J., and Thomas, K. M. (2001). A new species of *amphirhagatherium* (Choeropotamidae, artiodactyla, mammalia) from the late Eocene headon hill formation of southern england and phylogeny of endemic European 'anthracotherioids'. *Palaeontology* 44, 827–853. doi:10.1111/1475-4983.00203

Hooker, J. J., and Weidmann, M. (2000). The Eocene mammal faunas of Mormont, Switzerland: Systematic revision and resolution of dating problems. *Schweiz. Palaeontol. Abh.* 120, 1–143.

Janis, C., Effinger, J., Harrison, J., Honey, J., Kron, D., Lander, B., et al. (1998). "Artiodactyla," in *Evolution of tertiary mammals of North America*. Editors C. M. Janis, K. M. Scott, and L. L. Jacobs (Cambridge: Cambridge University Press), 337–357.

Jiang, H.-X. (1983). Division of the Paleogene in the Erlian Basin of inner Mongolia. *Geol. Inn. Mogolia* 2, 18–36.

Krause, D. W., and Maas, M. C. (1990). "The biogeographic origins of late Paleocene-early Eocene mammalian immigrants to the Western Interior of North America," in *Dawn of the age of mammals in the northern part of the rocky mountain interior*. Editors T. M. Bown and K. D. Rose North America (Boulder, Colorado: Geological Society of America Special Paper), 71–105.

Kumar, K., Rose, K. D., Rana, R. S., Singh, L., Smith, T., and Sahni, A. (2010). Early Eocene artiodactyls (mammalia) from Western India. *J. Vertebrate Paleontology* 30, 1245–1274. doi:10.1080/02724634.2010.483605

Lavocat, R. (1951). *Révision de la faune des mammifères oligocènes d'Auvergne et du Velay*. Paris: Science Avenir Editions.

Li, Q., and Li, Q. (2021). A new middle Eocene bunodont artiodactyl from the Erlian Basin (nei mongol, China). *Hist. Biol.* 34, 1941–1949. doi:10.1080/08912963.2021.1989679

Licht, A., Métais, G., Coster, P., İbilioğlu, D., Ocakoğlu, F., Westerweel, J., et al. (2022). Balkanatolia: The insular mammalian biogeographic province that partly paved the way to the Grande Coupure. *Earth-Science Rev.* 226, 103929. doi:10.1016/j.earscirev.2022.103929

Lucas, S. G., and Emry, R. J. (1996). Late Eocene entelodonts (mammalia: Artiodactyla) from inner Mongolia, China. *Proc. Biol. Soc. Wash.* 109, 397–405.

Luccisano, V., Sudre, J., and Lihoreau, F. (2020). Revision of the Eocene artiodactyls (mammalia, placentalia) from aumelas and saint-martin-de-londres (montpellier limestones, hérault, France) questions the early European artiodactyl radiation. *J. Syst. Palaeontol.* 18, 1631–1656. doi:10.1080/14772019.2020.1799253

Martinez, J. N., and Sudre, J. (1995). The astragalus of Paleogene artiodactyls–comparative morphology, variability and prediction of body-mass. *Lethaia* 28, 197–209. doi:10.1111/j.1502-3931.1995.tb01423.x

Matthew, W. D., and Granger, W. (1925a). New mammals from the Irdin Manha Eocene of Mongolia. *Am. Mus. Novit.* 198, 1–10.

Matthew, W. D., and Granger, W. (1925b). New mammals from the Shara Murun Eocene of Mongolia. *Am. Mus. Novit.* 196, 1–12.

Matthew, W. D., and Granger, W. (1923). *The fauna of the Houldjin gravels*. New York: American Museum of Natural History, 1–6.

McKenna, M. C., and Bell, S. K. (1997). *Classification of mammals above the species level.* New York: Columbia University Press.

McKenna, M. C. (1975). Fossil mammals and early Eocene north-atlantic land continuity. *Ann. Mo. Botanical Gard.* 62, 335–353. doi:10.2307/2395200

McKenna, M. C. (1983). Holarctic landmass rearrangement, cosmic events, and Cenozoic terrestrial organisms. *Ann. Mo. Botanical Gard.* 70, 459–489. doi:10.2307/2992083

Métais, G., Benammi, M., Chaimanee, Y., Jaeger, J.-J., Tun, T., Thein, T., et al. (2000). Discovery of new ruminant dental remains from the middle Eocene pondaung formation (Myanmar): Reassessment of the phylogenetic position of indomeryx. *Comptes Rendus de l'Académie des Sci. - Ser. IIA - Earth Planet. Sci.* 330, 805–811. doi:10.1016/s1251-8050(00)00184-1

Métais, G., Chaimanee, Y., Jaeger, J.-J., and Ducrocq, S. (2001). New remains of primitive ruminants from Thailand: Evidence of the early evolution of the Ruminantia in Asia. *Zool. Scr.* 30, 231–248. doi:10.1046/j.0300-3256.2001.00071.x

Métais, G., Coster, P. M., Kappelman, J. R., Licht, A., Ocakoğlu, F., Taylor, M. H., et al. (2018). Eocene metatherians from Anatolia illuminate the assembly of an island fauna during Deep Time. *PLoS ONE* 13, e0206181. doi:10.1371/journal.pone.0206181

Métais, G., Guo, J., and Beard, K. C. (2004). A new small dichobunid artiodactyl from Shanghuang (middle Eocene, eastern China): Implications for the early evolution of proto-selenodonts in Asia. *Bull. Carnegie Mus. Nat. Hist.* 36, 177–197. doi:10.2992/0145-9058(2004)36[177:ansdaf]2.0.co;2

Métais, G. (2006). New basal selenodont artiodactyls from the Pondaung Formation (late middle Eocene, Myanmar) and the phylogenetic relationships of early ruminants. *Ann. Carnegie Mus.* 75, 51–67. doi:10.2992/0097-4463(2006)75[51:nbsaft]2.0.co;2

Métais, G., Qi, T., Gu, J. W., and Beard, K. C. (2005). A new bunoselenodont artiodactyl from the Middle Eocene of China and the early record of selenodont artiodactyls in Asia. *J. Vertebrate Paleontology* 25, 994–997. doi:10.1671/0272-4634(2005)025[0994:anbaft]2.0.co;2

Métais, G., Qi, T., Guo, J. W., and Beard, K. C. (2008). Middle-eocene artiodactyls from Shanghuang (Jiangsu province, coastal China) and the diversity of basal dichobunoids in Asia. *Naturwissenschaften* 95, 1121–1135. doi:10.1007/s00114-008-0428-2

Métais, G., Soe, A. N., Marivaux, L., and Beard, K. C. (2007). Artiodactyls from the pondaung formation (Myanmar): New data and reevaluation of the south Asian faunal province during the middle Eocene. *Naturwissenschaften* 94, 759–768. doi:10.1007/s00114-007-0256-9

Métais, G., and Vislobokova, I. A. (2007). "Basal ruminants," in *The evolution of artiodactyls*. Editors D. R. Prothero and S. E. Foss (Baltimore: The Johns Hopkins University Press), 189–212.

Missiaen, P., and Gingerich, P. D. (2014). "New basal Perissodactyla (mammalia) from the lower Eocene ghazij formation of Pakistan," in *Contributions from the Museum of Paleontology* (Ann Arbor, Michigan: The University of Michigan), 32, 139–160.

Norris, C. A. (1999). The cranium of *Bunomeryx* (artiodactyla: Homacodontidae) from the upper Eocene uinta deposits of Utah and its implications for tylopod systematics. *J. Vertebrate Paleontology* 19, 742–751. doi:10.1080/02724634.1999.10011186

Orliac, M. J., and Ducrocq, S. (2012). Eocene raoellids (mammalia, cetartiodactyla) outside the Indian subcontinent: Palaeogeographical implications. *Geol. Mag.* 149, 80–92. doi:10.1017/s0016756811000586

Palcu, D. V., and Krijgsman, W. (2022). The dire straits of paratethys: Gateways to the anoxic giant of Eurasia. *Geol. Soc. Lond. Spec. Publ.* 523. in press. doi:10.1144/sp523-2021-73

Peterson, O. A. (1919). Report upon the material discovered in the upper Eocene of the uinta basin by earl douglas in the years 1908-1909, and by O. A. Peterson in 1912. *Ann. Carnegie Mus.* 12, 40–168. doi:10.5962/p.330969

Pickford, M., and Morales, J. (2003). New Listriodontinae (Mammalia, Suidae) from Europe and a review of listriodont evolution, biostratigraphy and biogeography. *Geodiversitas* 25, 347–404.

Rose, K. D. (1996). On the origin of the order artiodactyla. *Proc. Natl. Acad. Sci. U. S. A.* 93, 1705–1709. doi:10.1073/pnas.93.4.1705

Russell, D. E., and Zhai, R. J. (1987). The palaeogene of Asia: Mammals and stratigraphy. *Mémoires Du. Muséum Natl. d'Histoire Nat. Ser. C* 52, 1–488.

Schaeffer, B. (1947). Notes on the origin and function of the artiodactyl tarsus. *Am. Mus. Novitates* 1356, 1–24.

Simpson, G. G. (1945). The principles of classification and a classification of mammals. *Bull. Am. Mus. Nat. Hist.* 85, 1–350.

Sinclair, W. J. (1914). A revision of the bunodont artiodactyla of the middle and lower Eocene of North America. *Bull. Am. Mus. Nat. Hist.* 33, 267–295.

Singh Rana, R., Waqas, M., Orliac, M., Folie, A., and Smith, T. (2021). A new basal raoellid artiodactyl (mammalia) from the middle Eocene subathu group of rajouri district, Jammu and Kashmir, northwest himalaya, India. *Geobios* 66–67, 193–206. doi:10.1016/j.geobios.2020.12.003

Speijer, R. P., Pälike, H., Hollis, C. J., Hooker, J. J., and Ogg, J. G. (2020). "The Paleogene period," in *Geologic time scale 2020*. Editors F. M. Gradstein, J. G. Ogg, M. D. Schmitz, and G. M. Ogg (Amsterdam, Netherlands: Elsevier), 1087–1140.

Stehlin, H. G. (1910). Die Säugetiere des schweizerischen Eocaens, Sechster Teil: *Catodontherium–Dacrytherium–Leptotheridium–Anoplotherium–Diplobune–Xiphodon–Pseudamphimeryx–Amphimeryx–Dichodon–Haplomeryx–Tapirulus–Gelocus*–Nachträge–Artiodactyla incertae sedis–Schlussbetrachtungen über die Artiodactylen–Nachträge zu den Perissodactylen. *Abh. Schweiz. Palaeontologischen Ges.* 36, 838–1164.

Stehlin, H. G. (1906). Die Säugetiere des schweizerischen Eocaens, Vierter Teil: *Dichobune–Mouillacitherium–Meniscodon–Oxacron*. *Abh. Schweiz. Palaeontologischen Ges.* 33, 596–690.

Stucky, R. K. (1998). "Eocene bunodont and bunoselenodont Artiodactyla ("dichobunids")," in *Evolution of tertiary mammals of North America*. Editors C. M. Janis, K. M. Scott, and L. L. Jacobs (Cambridge: Cambridge University Press), 358–374.

Sudre, J., and Erfurt, J. (1996). Les artiodactyles du gisement yprésien terminal de Premontre (Aisne, France). *Palaeovertebrata* 25, 391–414.

Sudre, J. (1978). "Les Artiodactyles de l'Eocene moyen et superieur d'Europe occidentale (systematique et evolution)," in *Memoires et Travaux de l'institut de Montpellier de l'Ecole Pratique Des Hautes Etudes* (Montpellier: Ecole Pratique des Hautes Etudes, Institut de Montepellier), 7, 1–229.

Sudre, J. (1972). Révision des artiodactyles de l'Éocene moyen de Lissieu (Rhône). *Paleovertebrata* 5, 111–156.

Sudre, J., Russell, D. E., Louis, P., and Savage, D. E. (1983). Les artiodactyles de l'Eocene inferieur d'Europe (seconde partie). *Bull. Du. Mus. Natl. d'Histoire Nat.* 5, 339–365.

Theodor, J. M., Erfurt, J., and Métais, G. (2007). "The earliest artiodactyls: Diacodexeidae, Dichobunidae, Homacodontidae, leptochoeridae, and Raoellidae," in *The evolution of artiodactyls*. Editors D. R. Prothero and S. E. Foss (Baltimore: John Hopkins University Press), 32–58.

Theodor, J. M., Rose, K. D., and Erfurt, J. (2005). "Artiodactyla," in *The rise of placental mammals: Origins and relationships of the major extant clades*. Editors K. D. Rose and J. D. Archibald (Baltimore: Johns Hopkins University Press), 215–233.

Thewissen, J. G. M., Cooper, L. N., Clementz, M. T., Bajpai, S., and Tiwari, B. N. (2007). Whales originated from aquatic artiodactyls in the Eocene epoch of India. *Nature* 450, 1190–1194. doi:10.1038/nature06343

Thewissen, J. G. M., Gingerich, P. D., and Russell, D. E. (1987). "Artiodactyla and Perissodactyla (mammalia) from the early-middle Eocene kuldana formation of kohat (Pakistan)," in *Contributions from the Museum of Paleontology* (Ann Arbor, Michigan: The University of Michigan), 27, 247–274.

Thewissen, J. G. M., Nanda, A. C., and Bajpai, S. (2020). "*Indohyus*, endemic radiation of raoellid artiodactyls in the Eocene of India and Pakistan," in *Biological consequences of plate tectonics: New perspectives on post-gondwana break-up–A tribute to ashok sahni*. Editors G. V. R. Prasad and R. Patnaik (Cham: Springer International Publishing), 337–346.

Tissier, J., Becker, D., Codrea, V., Costeur, L., Fărcaş, C., Solomon, A., et al. (2018). New data on amynodontidae (mammalia, Perissodactyla) from eastern Europe: Phylogenetic and palaeobiogeographic implications around the eocene-oligocene transition. *PLoS ONE* 13, e0193774. doi:10.1371/journal.pone.0193774

Tsubamoto, T., Egi, N., Takai, M., Thaung, H., and Zin Maung Maung, T. (2013). A new genus and species of bunodont artiodactyl from the Eocene Pondaung Formation, Myanmar. *Paleontological Res.* 17, 297–311. doi:10.2517/1342-8144-17.4.297

Tsubamoto, T., Tun, S. T., Egi, N., Takai, M., Shigehara, N., Soe, A., et al. (2003). Reevaluation of some ungulate mammals from the Eocene pondaung formation, Myanmar. *Paleontological Res.* 7, 219–243. doi:10.2517/prpsj.7.219

Van der Made, J. G., and Han, D. (1994). Suoidea from the upper Miocene hominoid locality of Lufeng, Yunnan province, China. *Proc. Koninklijke Nederl. Akademie van Wetenschappen* 97, 27–82.

Van der Made, J. (1996). Listriodontinae (Suidae, Mammalia), their evolution, systematics and distribution in time and space. *Contributions Tert. Quat. Geol.* 33, 3–254.

Van der Made, J. (1997). Systematics and stratigraphy of the genera taucanamo and Schizochoerus and a classification of the palaeochoeridae (suoidea, mammalia). *Proc. Koninklijke Nederl. Akademie van Wetenschappen* 100, 127–139.

Viret, J. (1961). "Artiodactyla," in *Traité de Paléontologie*. Editor J. Piveteau (Paris: Masson et Cie), 887–1084.

Vislobokova, I. A. (2004b). A new representative of the family Raoellidae (suiformes) from the middle Eocene of khaichin-ula 2, Mongolia. *Paleontological J.* 38, 220–226.

Vislobokova, I. A. (1998). A new representative of the Hypertraguloidea (Tragulina, Ruminantia) from the Khoer-Dzan locality in Mongolia, with remarks on the relationships of the Hypertragulidae. *Am. Mus. Novitates* 3225, 1–24.

Vislobokova, I. A. (2002). *Archaeomeryx* (archaeomerycidae, Ruminantia): Morphology, ecology, and role in the evolution of the artiodactyla. *Paleontological J.* 36, S429–S522.

Vislobokova, I. A. (2004a). Artiodactyls from the middle Eocene of khaichin-ula II, Mongolia. *Paleontological J.* 38, 90–96.

Vislobokova, I. A. (2008). The oldest representative of Entelodontoidea (Artiodactyla, Suiformes) from the Middle Eocene of Khaichin Ula II, Mongolia, and some evolutionary features of this superfamily. *Paleontological J.* 42, 643–654. doi:10.1134/S0031030108060105

Wang, B. Y., and Qiu, Z. X. (2002). A new species of Entelodontidae (artiodactyla, mammalia) from late Eocene of Nei Mongol, China. *Vertebr. Palasiat.* 40, 194–202.

Wang, B. Y., Qiu, Z. X., Zhang, Q. Z., Wu, L. J., and Ning, P. J. (2009). Large mammals found from Houldjin formation near erenhot, nei mongol, China. *Vertebr. Palasiat.* 47, 85–110.

Wang, Y. Q., Li, Q., Bai, B., Jin, X., Mao, F. Y., and Meng, J. (2019). Paleogene integrative stratigraphy and timescale of China. *Sci. China Earth Sci.* 62, 287–309. doi:10.1007/s11430-018-9305-y

Wang, Y. Q., Meng, J., and Jin, X. (2012). Comments on Paleogene localities and stratigraphy in the Erlian Basin, nei mongol, China. *Vertebr. Palasiat.* 50, 181–203.

West, R. M. (1984). Paleontology and geology of the bridger formation, southern green river basin, souwester Wyoming, Part 7: Survey of bridgeran artiodactyla, including description of a skull and partial skeleton of *Antiacodon pygmaeus*. *Contributions Biol. Geol. Milwaukee Public Mus.* 56, 1–47.

Woodburne, M. O. (2004). "Global events and the North American mammalian biochronology," in *Late cretaceous and cenozoic mammals of North America*. Editor M. O. Woodburne (New York: Columbia University Press), 315–344.

Zhang, Y., Liu, Z., Fu, S., Jiang, S., Yao, N., and Wang, X. (2019). New understandings of the basement characteristics and evolution process of Erlian Basin. *Oil Geophys. Prospect.* 54, 404–416.